Table 1 Patient clinical characteristics and the therapeutic efficacy in 44 CH-B patients in relation to their baseline HBV DNA

	Baseline HBV DNA		
	<2.6 logcopies/ml ($n = 31$)	2.6–<4.0 logcopies/ml ($n = 7$)	≥4.0 logcopies/ml ($n = 6$)
At the commencement of switching treatment to entecavir			
Gender (male/female)	19/12	5/2	4/2
Age (years)	60 (35–79)[a]	65 (41–69)	55 (33–65)
HBeAg (positive/negative)	9/22	3/4	5/1[b]
HBV DNA (logcopies/ml)	<2.6	3.1 (2.6–3.6)[c]	4.6 (4.0–5.2)[c,d]
rtM204V/I mutation (absence/NT)	23/8	5/2	5/1
ALT (IU/l)	25 (11–64)	31 (13–46)	20 (17–78)
Chronic hepatitis/cirrhosis/HCC	19/7/5	4/2/1	4/2/0
Follow-up period of entecavir treatment (months)	19 (10–23)	19 (10–22)	20 (16–22)
The rate of undetectable HBV DNA level during follow-up	31 (100%)	7 (100%)	3 (50%)[c]
Emergence of entecavir-resistance during follow-up	0 (0%)	0 (0%)	1 (17%)
At the commencement of preceding lamivudine treatment			
HBeAg (positive/negative)	12/19	4/3	5/1
HBV DNA (logcopies/ml)	6.5 (4.3–7.6‹)	6:6 (6.2–7.6‹)	7.6‹ (5.9–7.6‹)
Duration of preceding lamivudine treatment (months)	15 (6–73)	10 (7–42)	9 (8–32)

NT not tested

[a] Values are expressed as median (range)

[b] $p < .05$ versus baseline HBV DNA <2.6 logcopies/ml group

[c] $p < .01$ versus baseline HBV DNA <2.6 logcopies/ml group

[d] $p < .01$ versus baseline HBV DNA of 2.6–<4.0 logcopies/ml group

follow-up period of entecavir treatment did not differ among the three groups. Also, there was no significant difference in HBV DNA and the frequency of positive HBeAg at the commencement of preceding lamivudine treatment among them.

Antiviral efficacy and drug resistance in lamivudine-to-entecavir switching treatment in relation to baseline HBV DNA

Next, we investigated serial changes in HBV DNA after the switch from lamivudine to entecavir treatment in CH-B patients in relation to the baseline HBV DNA. All 31 patients with baseline HBV DNA <2.6 logcopies/ml maintained undetectable HBV DNA during the follow-up period of entecavir treatment. Figure 1 shows the longitudinal evaluation of HBV DNA during the switching treatment to entecavir in patients with a detectable level of baseline HBV DNA. In patients having baseline HBV DNA of 2.6–<4.0 logcopies/ml (Fig. 1a), all of the seven patients achieved sustained undetectable HBV DNA during follow-up, although HBV DNA was transiently detected in one patient. As for patients having baseline HBV DNA ≥4.0 logcopies/ml (Fig. 1b), three (50%) of the six patients achieved sustained undetectable HBV DNA during follow-up. In two patients, HBV DNA was not cleared entirely, but declined to 2.9 and 2.7 logcopies/ml at month 18, respectively. In sequencing analysis at that time, the former patient had the lamivudine-resistant rtM204I substitution, although it was not detected by the PCR–ELMA assay at the start of entecavir treatment. The latter patient had no drug resistance-associated substitutions. In the sixth patient, HBV DNA decreased initially, but virological breakthrough was seen at month 15. The entecavir-resistant virus was detected after virological breakthrough. The detailed disease course of the entecavir-resistant patient is described below. As for the relationship of baseline HBV DNA to the frequency of undetectable HBV DNA, HBV DNA was cleared more frequently in patients with baseline HBV DNA <2.6 logcopies/ml than in those with baseline HBV DNA ≥4.0 logcopies/ml (100 vs. 50%, $p < .01$) (Table 1).

Serial changes in ALT during lamivudine-to-entecavir switching treatment were further examined. Among the 31 patients with baseline HBV DNA <2.6 logcopies/ml, the baseline ALT was within the normal range (≤40 IU/l) in 27 patients, 24 of whom showed sustained ALT normalization during follow-up. In the remaining three patients, ALT became slightly abnormal (≤60 IU/l) during follow-up. As for four patients with abnormal baseline ALT, the level was normalized in three, whereas a slight elevation of ALT (≤60 IU/l) continued in one during follow-up.

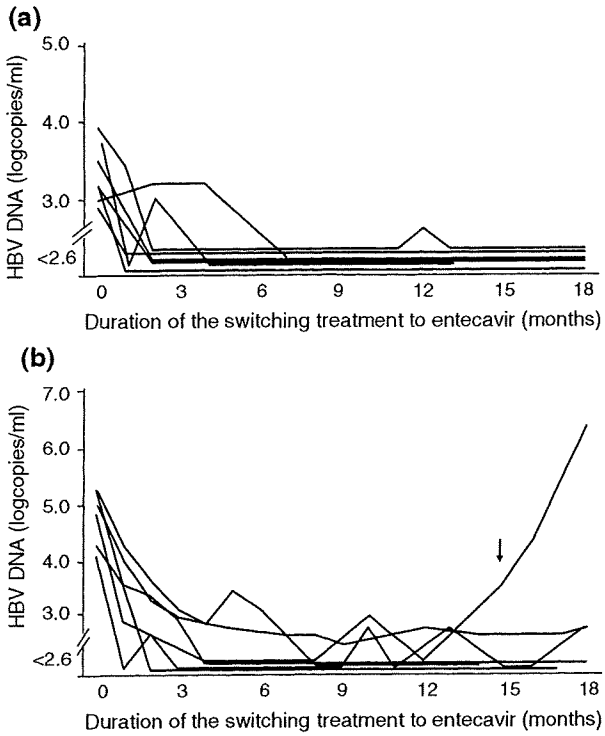

Fig. 1 Changes in HBV DNA after commencement of switching treatment from lamivudine to entecavir in CH-B patients with baseline HBV of (**a**) 2.6–<4.0 logcopies/ml and (**b**) ≥4.0 logcopies/ml. The *black arrow* indicates the time point of virological breakthrough

Among the 13 patients having a detectable level of baseline HBV DNA, five patients (three with baseline HBV DNA of 2.6–<4.0 logcopies/ml and two with baseline HBV DNA ≥4.0 logcopies/ml) had abnormal ALT at baseline but showed ALT normalization during follow-up. In the remaining eight patients, ALT continued to be normal from the beginning of entecavir treatment.

Disease course of the CH-B patients showing entecavir-resistance during lamivudine-to-entecavir switching treatment

The disease course of the entecavir-resistant patient is shown in Fig. 2. This patient was a 33-year-old HBeAg-positive male, whose liver biopsy showed features of chronic hepatitis. He underwent the preceding lamivudine treatment for 8 months. HBV DNA decreased from >7.6 to 4.6 logcopies/ml, and ALT was normalized during the lamivudine therapy. The rtM204V/I substitution was not detected before the switch to entecavir treatment by the PCR–ELMA analysis. After the commencement of entecavir treatment, HBV DNA was cleared at month 5. However, virological breakthrough was seen at month 15, and HBV DNA was further increased to 6.1 logcopies/ml at month 18. The sequencing analysis at month 18 revealed the rtM204V, rtL180M and rtS202G substitutions. Two additional substitutions, rtL267M and rtQ316H, were also found, when the amino acid sequences were compared with three representative genotype C HBV isolates (Genbank accession nos. V00867, X01587 and D00630) [21–23]. Breakthrough hepatitis was not evident after the emergence of entecavir-resistant mutant virus. The sequencing analysis also revealed that he was infected with HBV of genotype C.

Discussion

Entecavir treatment has been shown to exhibit more powerful antiviral efficacy and less frequent drug resistance than lamivudine treatment in nucleos(t)ide analog-naïve CH-B patients [14, 15, 17]. Entecavir is also effective in patients showing lamivudine resistance during the preceding lamivudine treatment, but its efficacy is limited due to the higher incidence of entecavir-resistance, compared with nucleos(t)ide analog-naïve ones [16, 17]. This is because entecavir-resistance is established based on two lamivudine-resistant substitutions, rtM204V and rtL180M, and additional mutation(s) occurring at rt184, rt202 and/or rt250 [18]. A considerable number of CH-B patients remain under continuous lamivudine treatment, while the lamivudine-to-entecavir switching treatment could yield a practical benefit. The switching treatment may be more promising for patients before the appearance of lamivudine resistance than after its development. In the present study, we investigated the efficacy of lamivudine-to-entecavir switching treatment in CH-B patients without apparent evidence of lamivudine resistance during the preceding lamivudine treatment.

We evaluated the antiviral efficacy of the switching treatment to entecavir in relation to the baseline HBV DNA at the commencement of the entecavir administration. In all patients having baseline HBV DNA <2.6 logcopies/ml, who revealed a good response to the preceding lamivudine treatment, HBV DNA continued to be undetectable during the switching treatment to entecavir. Also, all patients having baseline HBV DNA of 2.6–<4.0 logcopies/ml achieved sustained undetectable HBV DNA during the follow-up period of entecavir treatment. Among six patients having baseline HBV DNA ≥4.0 logcopies/ml, who did not respond well to the preceding lamivudine treatment, HBV DNA was cleared in three during follow-up. Its reduction by up to 3.0 logcopies/ml was seen in two additional cases without emergence of the entecavir-resistant virus. Thus, the antiviral efficacy of the lamivudine-to-entecavir switching treatment was exhibited in almost all CH-B patients in parallel with that of the preceding

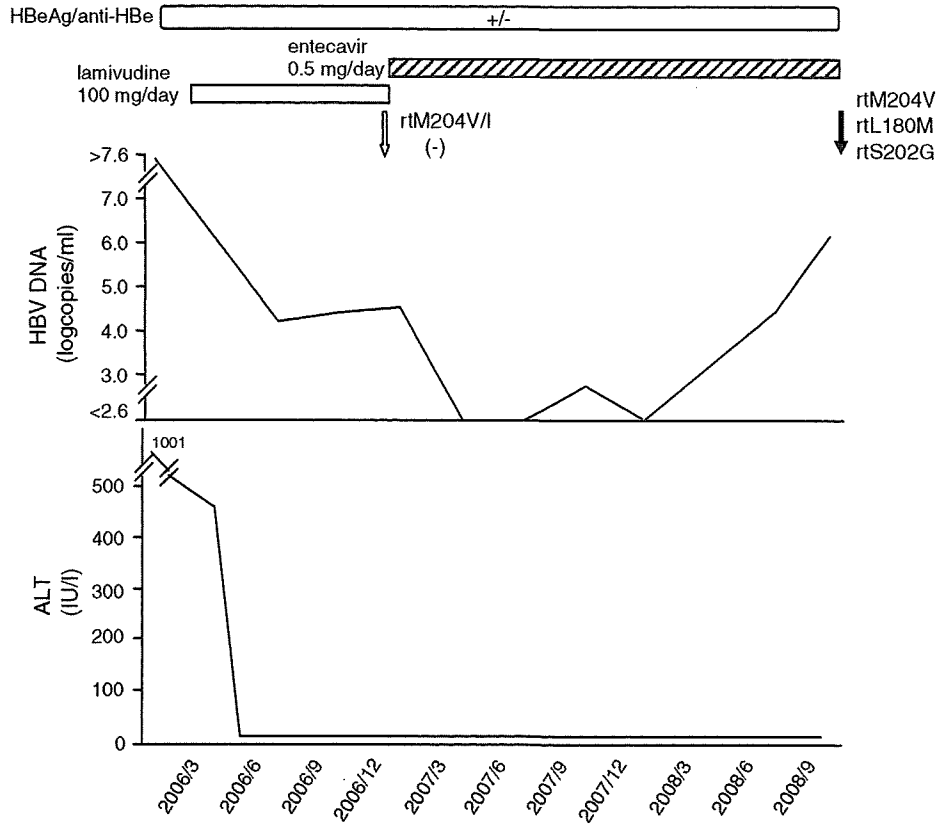

Fig. 2 Disease course of the CH-B patient showing entecavir-resistance during switching treatment to entecavir. The *white arrow* indicates the time point of the PCR–ELMA assay to detect rtM204V/I mutation, whereas the *black arrow* indicates the time point of the PCR-direct sequencing analysis

lamivudine treatment. In addition, the switching treatment to entecavir tended to yield a greater decrease in HBV DNA than the preceding lamivudine treatment. These results indicate that the switch from lamivudine to entecavir may be generally recommendable compared with continuation of lamivudine administration in CH-B patients without evidence of lamivudine resistance.

In this study, one of the six patients having baseline HBV DNA ≥4.0 logcopies/ml showed entecavir-resistance during the switching treatment to entecavir. It was probably due to the existence of an extremely small amount of lamivudine-resistant virus mixed with a predominant wild-type virus, which could not be detected by the sensitive PCR–ELMA assay at the start of the switch to entecavir treatment. It is speculated that, during entecavir treatment, the lamivudine-resistant virus having rtM204V and rtL180M substitutions may become predominant with time, followed by the establishment of entecavir-resistant virus via the additional rtS202G substitution. Compared to the low incidence of drug resistance in entecavir treatment for nucleos(t)ide analog-naïve CH-B patients [17], the entecavir-resistance may occur more frequently in the lamivudine-to-entecavir switching treatment for patients without evidence of lamivudine resistance. In particular, patients who do not achieve a good response to the preceding lamivudine treatment are speculated to have a higher risk for the development of entecavir-resistance in the switching treatment to entecavir, although it should be verified by further studies.

In conclusion, in CH-B patients receiving the continuous lamivudine treatment, it may be recommendable to switch to entecavir treatment before the appearance of lamivudine resistance. It may contribute to reducing the subsequent emergence of drug resistance. However, great care should be taken with respect to the emergence of entecavir-resistant virus after the switch to entecavir treatment, especially in patients who do not respond well to the preceding lamivudine treatment. Our retrospective study with a small number of patients and a short duration of follow-up cannot draw a definite conclusion but still provides some information about the clinical possibilities of the lamivudine-to-entecavir switching treatment. Further detailed investigation with a larger number of patients and a longer follow-up period may offer better understanding.

References

1. Lai CL, Chien RN, Leung NW, Chang TT, Guan R, Tai DI, et al. A one-year trial of lamivudine for chronic hepatitis B. Asia Hepatitis Lamivudine Study Group. N Engl J Med. 1998;339:61–8.
2. Dienstag JL, Schiff ER, Wright TL, Perrillo RP, Hann HW, Goodman Z, et al. Lamivudine as initial treatment for chronic

hepatitis B in the United States. N Engl J Med. 1999;341:1256–63.
3. Lai CL, Dienstag J, Schiff E, Leung NW, Atkins M, Hunt C, et al. Prevalence and clinical correlates of YMDD variants during lamivudine therapy for patients with chronic hepatitis B. Clin Infect Dis. 2003;36:687–96.
4. Allen MI, Deslauriers M, Andrews CW, Tipples GA, Walters KA, Tyrrell DL, et al. Identification and characterization of mutations in hepatitis B virus resistant to lamivudine. Lamivudine Clinical Investigation Group. Hepatology. 1998;27:1670–7.
5. Liaw YF, Chien RN, Yeh CT, Tsai SL, Chu CM. Acute exacerbation and hepatitis B virus clearance after emergence of YMDD motif mutation during lamivudine therapy. Hepatology. 1999;30:567–72.
6. Westland CE, Yang H, Delaney WE 4th, Wulfsohn M, Lama N, Gibbs CS, et al. Activity of adefovir dipivoxil against all patterns of lamivudine-resistant hepatitis B viruses in patients. J Viral Hepat. 2005;12:67–73.
7. Ono-Nita SK, Kato N, Shiratori Y, Lan KH, Yoshida H, Carrilho FJ, et al. Susceptibility of lamivudine-resistant hepatitis B virus to other reverse transcriptase inhibitors. J Clin Invest. 1999; 103:1635–40.
8. Hadziyannis SJ, Tassopoulos NC, Heathcote EJ, Chang TT, Kitis G, Rizzetto M, et al. Adefovir dipivoxil for the treatment of hepatitis B e antigen-negative chronic hepatitis B. N Engl J Med. 2003;348:800–7.
9. Marcellin P, Chang TT, Lim SG, Tong MJ, Sievert W, Shiffman ML, et al. Adefovir dipivoxil for the treatment of hepatitis B e antigen-positive chronic hepatitis B. N Engl J Med. 2003; 348:808–16.
10. Perrillo R, Hann HW, Mutimer D, Willems B, Leung N, Lee WM, et al. Adefovir dipivoxil added to ongoing lamivudine in chronic hepatitis B with YMDD mutant hepatitis B virus. Gastroenterology. 2004;126:81–90.
11. Peters MG, Hann Hw H, Martin P, Heathcote EJ, Buggisch P, Rubin R, et al. Adefovir dipivoxil alone or in combination with lamivudine in patients with lamivudine-resistant chronic hepatitis B. Gastroenterology. 2004;126:91–101.
12. van Bömmel F, Wünsche T, Mauss S, Reinke P, Bergk A, Schürmann D, et al. Comparison of adefovir and tenofovir in the treatment of lamivudine-resistant hepatitis B virus infection. Hepatology. 2004;40:1421–5.
13. van Bömmel F, Zöllner B, Sarrazin C, Spengler U, Hüppe D, Möller B, et al. Tenofovir for patients with lamivudine-resistant hepatitis B virus (HBV) infection and high HBV DNA level during adefovir therapy. Hepatology. 2006;44:318–25.
14. Chang TT, Gish RG, de Man R, Gadano A, Sollano J, Chao YC, et al. A comparison of entecavir and lamivudine for HBeAg-positive chronic hepatitis B. N Engl J Med. 2006;354:1001–10.
15. Lai CL, Shouval D, Lok AS, Chang TT, Cheinquer H, Goodman Z, et al. Entecavir versus lamivudine for patients with HBeAg-negative chronic hepatitis B. N Engl J Med. 2006;354:1011–20.
16. Sherman M, Yurdaydin C, Sollano J, Silva M, Liaw YF, Cianciara J, et al. Entecavir for treatment of lamivudine-refractory, HBeAg-positive chronic hepatitis B. Gastroenterology. 2006;130:2039–49.
17. Colonno RJ, Rose R, Pokornowski K, Baldick C, Eggers B, Yu D, et al. Four year assessment of ETV resistance in nucleoside-naïve and lamivudine refractory patients. J Hepatol. 2007; 46:S294. (Abst.).
18. Tenney DJ, Rose RE, Baldick CJ, Levine SM, Pokornowski KA, Walsh AW, et al. Two-year assessment of entecavir resistance in Lamivudine-refractory hepatitis B virus patients reveals different clinical outcomes depending on the resistance substitutions present. Antimicrob Agents Chemother. 2007;51:902–11.
19. Levine S, Hernandez D, Yamanaka G, Zhang S, Rose R, Weinheimer S, et al. Efficacies of entecavir against lamivudine-resistant hepatitis B virus replication and recombinant polymerases in vitro. Antimicrob Agents Chemother. 2002;46:2525–32.
20. Kobayashi S, Ide T, Sata M. Detection of YMDD motif mutations in some lamivudine-untreated asymptomatic hepatitis B virus carriers. J Hepatol. 2001;34:584–6.
21. Ono Y, Onda H, Sasada R, Igarashi K, Sugino Y, Nishioka K. The complete nucleotide sequences of the cloned hepatitis B virus DNA; subtype adr and adw. Nucleic Acids Res. 1983; 11:1747–57.
22. Fujiyama A, Miyanohara A, Nozaki C, Toneyama T, Ohtomo N, Matsubara K. Cloning and structural analyses of hepatitis B DNAs, subtype *adr*. Nucleic Acids Res. 1983;11:4601–10.
23. Kobayashi M, Koike K. Complete nucleotide sequence of hepatitis B virus DNA of subtype adr and its conserved gene organization. Gene. 1984;30:227–32.

Journal of Viral Hepatitis, 2009, 16, 844–852 doi:10.1111/j.1365-2893.2009.01131.x

Enhanced ability of regulatory T cells in chronic hepatitis C patients with persistently normal alanine aminotransferase levels than those with active hepatitis

I. Itose,[1] T. Kanto,[1] N. Kakita,[1] S. Takebe,[1] M. Inoue,[1] K. Higashitani,[1] M. Miyazaki,[1] H. Miyatake,[1] M. Sakakibara,[1] N. Hiramatsu,[1] T. Takehara,[1] A. Kasahara[2] and N. Hayashi[1]

[1]*Department of Gastroenterology and Hepatology, Osaka University Graduate School of Medicine, Suita, Japan; and* [2]*Department of General Medicine, Osaka University Hospital, Suita, Japan*

Received December 2008; accepted for publication February 2009

SUMMARY. In hepatitis C virus (HCV) infection, the Th1-type immune response is involved in liver injury. A predominance of immunosuppressive regulatory T cells (Treg) is hypothesized in patients with persistently normal alanine aminotransferase (PNALT). Our aim was to clarify the role of Treg in the pathogenesis of PNALT. Fifteen chronically HCV-infected patients with PNALT, 21 with elevated ALT (CH) and 19 healthy subjects (HS) were enrolled. We determined naturally-occurring Treg (N-Treg) as CD4+CD25high+ FOXP3+ T cells. The expression of FOXP3 and CTLA4 in CD4+CD25high+ cells was quantified by real-time reverse transcriptase-polymerase chain reaction. Bulk or CD25-depleted CD4+ T cells cultured with HCV-NS5 loaded dendritic cells were assayed for their proliferation and cytokine release. We examined CD127–CD25–FOXP3+ cells as distinct subsets other than CD25+ N-Treg. The frequencies of N-Treg in patients were significantly higher than those in HS. The FOXP3 and CTLA4 transcripts were higher in PNALT than those in CH. The depletion of CD25+ cells enhanced HCV-specific T cell responses, showing that co-existing CD25+ cells are suppressive. Such inhibitory capacity was more potent in PNALT. The frequency of CD4+CD127–CD25–FOXP3+ cells was higher in CH than those in PNALT. Treg are more abundant in HCV-infected patients, and their suppressor ability is more potent in patients with PNALT than in those with active hepatitis.

Keywords: HCV, PNALT, regulatory T cell.

INTRODUCTION

Hepatitis C virus (HCV) causes a wide range of chronic liver diseases in infected hosts, including chronic hepatitis (CH), liver cirrhosis and hepatocellular carcinoma (HCC).

Abbreviations: ALT, alanine aminotransferase; CH, chronic hepatitis; CTL, cytotoxic T lymphocyte; DC, dendritic cell; ELISA, enzyme-linked immunosorbent assay; FACS, fluorescence-activated cell sorting; FBS, fetal bovine serum; HBV, hepatitis B virus; HCC, hepatocellular carcinoma; HCV, hepatitis C virus; HS, healthy subjects; IFN, interferon; IL, interleukin; IU, international units; MoDC, monocyte-derived dendritic cell; N-Treg, naturally occurring regulatory T cell; PNALT, persistently normal ALT; RT-PCR, reverse transcriptase-polymerase chain reaction; SLE, systemic lupus erythematosus; TGF, transforming growth factor; Treg, regulatory T cell.

Correspondence: Norio Hayashi, MD, PhD, Department of Gastroenterology and Hepatology, Osaka University Graduate School of Medicine, 2-2 Yamadaoka, Suita, Japan. E-mail: hayashin@gh.med.osaka-u.ac.jp

One of the critical determinants promoting the development of HCV-induced liver disease is sustained liver inflammation, explaining the therapeutic rationale of alleviating this condition to help prevent liver cancer [1]. Among chronically infected individuals, approximately 20–30% display persistently normal serum alanine aminotransferase levels [2,3]. Although it is reported that 40–50% of them progress to the active stage of liver inflammation within 5 years of observation [4], the incidence of HCC in the remaining patients continues to be lower than in those with elevated serum ALT levels [5]. Cumulative studies have revealed that HCV is not directly cytopathic to hepatocytes. It has been demonstrated that a Th1-type or cytotoxic T lymphocyte (CTL) response is critically involved in HCV-mediated liver injury [6,7]. Therefore, it is conceivable that some suppressor mechanisms exist against Th1-type immune responses in patients with persistently normal ALT levels (PNALT), which may be distinct from those in patients with active liver inflammation.

Regulatory T cells (Treg) are a unique subset of T cells with inhibitory capacity against auto-reactive T cells [8]. Substantial data have been reported about the involvement of Treg in the pathogenesis of various diseases, including autoimmune, cancer or infectious diseases [9–13]. Currently, the existence of several types of Treg has been reported [14]. Naturally occurring Treg (N-Treg) are derived from the thymic stromal environment from progenitor cells and suppress auto-reactive T cells in antigen-specific and antigen-nonspecific manner. Forkhead/winged helix transcription factor (FOXP3) is one of the specific markers of N-Treg, the expression of which is well correlated with the gain of a suppressor function [15,16]. As cells with high expression of CD25 also display FOXP3, it is generally accepted that CD25+FOXP3+ is the most reliable marker for Treg. In HCV infection, several reports have described a higher frequency of N-Treg in the periphery and the liver [17–20], suggesting their active role in HCV persistence. It has also been demonstrated that CD25+FOXP3+ regulatory cells are inducible in the periphery [21]. Owing to the lack of a specific phenotypic marker of these induced regulatory cells, referred to as adaptive Treg, their role in the pathogenesis of HCV infection has not been clearly understood. A recent study has demonstrated that the expression of interleukin (IL)-7 receptor (CD127) is downregulated in Treg to a degree that is inversely correlated with FOXP3 expression [22]. These findings offer the possibility that adaptive Treg are traceable, not all but in part, by the combination of CD127 and FOXP3 independent of CD25 expression.

In this study, our aim was to elucidate whether or not Treg are involved in the pathogenesis of PNALT patients, by comparing the frequency and function of these cell subsets with those in active hepatitis patients or healthy subjects. A distinct equilibrium was found between N-Treg and CD127–CD25–FOXP3+ T cells according to differences in liver inflammation.

MATERIALS AND METHODS

Subjects

Among chronically HCV-infected patients who had been followed at Osaka University Hospital, 15 patients with PNALT levels and 21 patients with elevated or fluctuating ALT levels (the CH group) were enrolled in this study. As controls, 19 healthy subjects (HS) who were negative for HCV and hepatitis B virus (HBV) markers were examined. The study protocol was approved by the ethical committee of Osaka University Graduate School of Medicine. At enrolment, written informed consent was obtained from each subject. In this study, PNALT patients were defined as those whose ALT levels remained within the normal range (<30 IU/mL) without any medications for more than 1 year. At enrolment, the patients were confirmed to be positive for both serum anti-HCV and HCV RNA, but were negative for other viral infections, including HBV and human immunodeficiency virus. The presence of other causes of liver disease, such as autoimmune, alcoholic and metabolic disorders was excluded by the use of laboratory and imaging analyses. Liver biopsy was carried out in some of the patients. Histological examination was performed according to the METAVIR scoring system. In all patients, a combination of repetitive biochemical tests, ultrasonography or computed tomography scans ruled out the presence of cirrhosis and liver tumours. The clinical background of the subjects are shown in Table 1.

Table 1 Baseline clinical characteristics of the patients

	Chronic hepatitis patients	Patients with PNALT	Healthy subjects*	
n	21	15	19	
Sex (M/F)	8/13	5/10	ND	NS
Age	50.6 ± 11.6	47.8 ± 12.7	ND	NS
ALT (IU/L)	88.3 ± 41.4	20.9 ± 6.9	ND	$P < 0.0001^{\dagger}$
Plt ($10^4/\mu L$)	13.5 ± 5.4	20.0 ± 3.9	ND	$P < 0.01^{\dagger}$
HCV RNA (Meq/mL)	8.6 ± 11.3	9.7 ± 7.8	ND	NS

*The background data of healthy subjects (blood donors) were not accessible owing to the confidentiality regulations of the blood centre, but their serum ALT levels were confirmed to be within the normal range. †Statistical significance was analysed by Mann–Whitney *U* test between chronic hepatitis patients and patients with PNALT. The values are expressed as mean ± SD. PNALT, persistently normal alanine aminotransferase level; ND, not determined; NS, not significant; plt, platelet count.

Frequency analyses of Treg cells

For the numerical analyses of Treg cells, heparinized venous blood was obtained from all subjects. Peripheral blood mononuclear cells were collected by density-gradient centrifugation on a Ficoll–Hypaque cushion. The cells were subsequently stained with a combination of various fluorescence-labelled anti-human mouse monoclonal antibodies for phenotypic markers. The antibodies for CD25 (clone B1.49.9) and CD4 (clone 13B8.2) were purchased from Beckman Coulter (Fullerton, CA, USA), that for CD127 (clone 40131) from R&D Systems (Minneapolis, MN, USA) and that for FOXP3-PE (clone PCH101) from eBioscience (San Diego, CA, USA), respectively. The cells were stained in phosphate-buffered saline containing 1% fetal bovine serum (FBS) with various antibodies or isotype controls for 15 min at room temperature. Intracellular staining of FOXP3 was performed using a human FOXP3 staining kit (eBioscience) according to the manufacturer's instructions. The cells were analysed by FACSCalibur (BD Biosciences, San Jose, CA, USA) and CellQuest software.

Functional analysis of CD4+CD25+ T cells in HCV-specific CD4+ T cell response

We first examined the HCV-specific CD4+ T cell response in the presence or absence of CD4+CD25+ T cells. Monocyte-derived dendritic cells (MoDC) were generated from CD14+ cells as reported previously. In brief, CD14+ cells were cultured in Iscove's modified Dulbecco's medium (Gibco Laboratories, Grand Island, NY, USA) supplemented with 10% FBS, 50 IU/mL of penicillin, 50 mg/mL of streptomycin, 2 mM of L-glutamine, 10 mM of Hepes buffer, 10 mM of nonessential amino acids in the presence of 50 ng/mL of granulocyte/macrophage colony-stimulating factor (PeproTech, Rocky Hill, NJ, USA) and 10 ng/mL of IL-4 (PeproTech) for 7 days at 37 °C and 5% CO_2. On day 6 of the culture, MoDC were pulsed with 10 μg/mL of recombinant HCV NS5 (amino acid position: NS5B 1-544; kindly provided by Japan Tobacco, Inc., Tokyo, Japan) and cultured for 24 h. The antigen-pulsed MoDC were then cultured with autologous bulk CD4+ T cells or CD4+CD25– T cells in 96-well flat-bottom plates (Corning, NY, USA) for 5 days. Enrichment of CD4+ T cells or CD4+CD25– T cells was performed using a CD4+CD25+ Regulatory T cell Isolation kit (Miltenyi Biotec, Auburn, CA, USA) according to the manufacturer's instructions. On day 6 of the co-culture, the cells were pulsed with 1 μCi of [3H]-thymidine during the last 16 h of incubation. The supernatants were collected before pulsing with [3H]-thymidine and subjected to cytokine enzyme-linked immunosorbent assay (ELISA). The incorporation of [3H]-thymidine in CD4+ T cells was measured using a β-counter (Wallac-Perkin-Elmer, Wallac, Finland).

Enzyme-linked immunosorbent assay

The concentrations of IL-10, TGF-β1 and interferon (IFN)-γ in the culture supernatants were determined by ELISA. We used matched pairs of relevant monoclonal antibodies (Endogen, Woburn, MA, USA) for IL-10 and IFN-γ, and the DuoSet ELISA development system (R&D Systems) for TGF-β1, according to the manufacturer's instructions. The detection thresholds of IL-10, TGF-β1 and IFN-γ were 10, 10 and 16 pg/mL, respectively.

Real time reverse transcriptase-polymerase chain reaction (RT-PCR)

In order to analyse the expression of FOXP3 and CTLA-4 in N-Treg, we collected CD4+CD25high T cells by using FACSAria. The purity of the isolated cells was more than 95% as determined by FACS. Total RNA was extracted from sorted CD4+CD25high T cells using the RNeasy Mini Kit (Qiagen, Valencia, CA, USA) according to the manufacturer's instructions. Complementary DNA was synthesized using the SuperScript III First-Strand synthesis system (Invitrogen, Carlsbad, CA, USA). Assays-on-demand primers and probes (PE Applied Biosystems, Foster City, CA, USA) were used to quantify FOXP3 and CTLA4 expression. The mRNA levels were evaluated using ABI PRISM 7900 Sequence Detection System (Applied Biosystems). The thermal cycling conditions for all genes were as follows: the reaction was started with a 10-min denaturing cycle at 95 °C, followed by 40 cycles of PCR performed with 15 s of denaturing at 95 °C, then 1 minute at 60 °C for annealing and extension. We identified a calibrator sample from the healthy volunteers. The expressions of molecules were given as the relative values to the calibrator samples. To standardize the amount of total RNA added to each reaction mixture, we quantified β-actin mRNA from each sample as a control of internal RNA and corrected all values with this.

Statistical analysis

Statistical analyses were performed using StatView 5.0 software (SAS Institute Inc., Cary, NC, USA). Mann–Whitney *U*-test was used to compare differences in unpaired samples. For all analyses, a *P*-value of less than 0.05 was considered to be statistically significant.

RESULTS

Peripheral N-Treg are increased in HCV-infected patients

We compared the frequency of Treg between HCV-infected patients and healthy donors. In HCV-positive individuals, they were further categorized into PNALT and CH groups according to the difference in their serum ALT levels. The clinical backgrounds of these groups were not different except for

serum ALT levels and platelet counts (Table 1). N-Treg were defined as the cells with CD4+CD25high+FOXP3+ cells. As the cut-off value between CD25high+ and CD25intermediate+ cells is a critical determinant for Treg analyses, we defined CD4+CD25high+ as the cells with CD25 levels higher than those of CD4–CD25+ cells (Fig. 1a). We first compared the frequency of CD4+FOXP3+ T cells. The frequency of FOXP3+ cells in the CD4+ T cell population in HCV-infected patients was significantly higher than those in the HS (Fig. 1b). However, no difference was observed in FOXP3+ cells between the PNALT and CH patients (Fig. 1b). The frequency of CD4+CD25high+FOXP3+ T cells in CH or PNALT patients were significantly higher than those in HS, whereas those in HCV-positive patients did not differ regardless of their ALT levels (Fig. 1c). Similar results were obtained for the frequency of CD4+CD25–FOXP3+ T cells (Fig. 1d).

Next, we examined whether or not the frequency of N-Treg is correlated with clinical parameters. Among all HCV-infected patients, no correlation was observed between the frequency of N-Treg (CD4+CD25high+ FOXP3+ T cells) and serum ALT, HCV RNA levels, age or platelet counts (data not shown). In the analyses of patients who had undergone liver biopsy, the frequency of N-Treg was not correlated with METAVIR grade/stage scores (data not shown).

The expressions of FOXP3 and CTLA4 are higher in N-Treg from PNALT patients compared with those from the CH group

FOXP3 is the master gene of Treg in the development and gaining of suppressor functions. Alternatively, CTLA4 is one of the key molecules of Treg in exerting inhibitory function. We thus evaluated FOXP3 and CTLA4 mRNA expression in sorted N-Treg (CD4+CD25high+ T cells) by means of real-time RT-PCR. The expression of FOXP3 in PNALT or CH patients was significantly higher than those in HS (Fig. 2a). Of note is the higher expression of FOXP3 in N-Treg from the PNALT group than in those from the CH group (Fig. 2a). In contrast, the expression of CTLA4 in N-Treg from the PNALT was higher than those in the CH, while it did not differ between the CH and HS groups (Fig. 2b).

CD4+CD25+ T cells from PNALT patients have more suppressive capacity in the HCV-specific CD4+ T cell response than those from CH patients

In order to compare the ability of N-Treg to inhibit the antigen-specific CD4+ T cell response, we used autologous MoDC pulsed with HCV proteins as antigen-presenting cells. We examined CD4+ T cell proliferation or cytokine

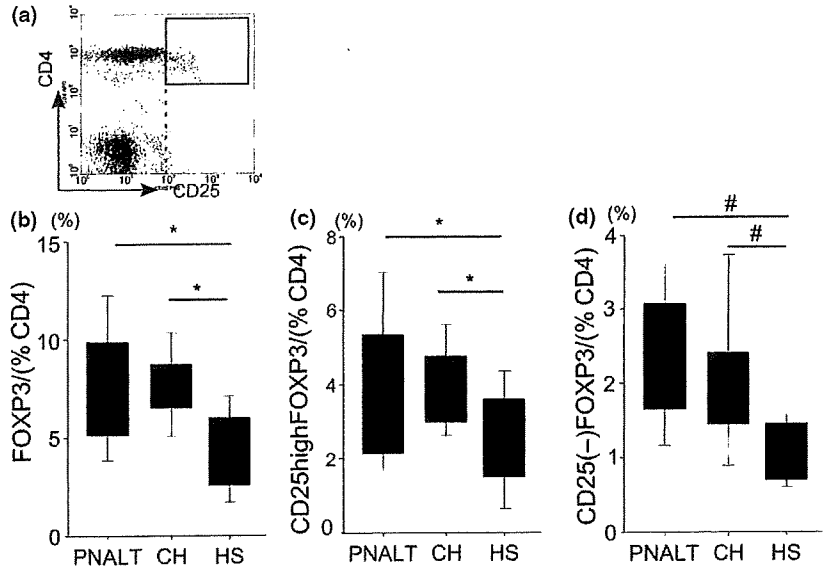

Fig. 1 Comparison of frequencies of naturally-occurring regulatory T cells (N-Treg) and FOXP3-positive cells among the groups. (a) Gating of CD4+CD25high+ T cells under FACS analysis. The cut-off value of CD25high expression is set at a level that is more than that of CD4–CD25+ cells (dotted line); CD4+CD25high+ T cells are shown in the rectangle drawn in the representative dot plot. (b) Frequencies of FOXP3+ cells, (c) N-Treg (CD25high+FOXP3+ cells) and (d) CD25–FOXP3+ cells in CD4+ T cells were compared among the groups. Boxes represent lower and upper quartiles with the median value (solid line) between boxes, while the whiskers represent the minimum and maximum values. *, $P < 0.05$; , $P < 0.0001$ by Mann–Whitney *U*-test. *Abbreviations:* PNALT, hepatitis C virus (HCV)-infected patients with persistently normal alanine aminotransferase (ALT) levels; CH, HCV-infected patients with elevated ALT levels; HS, healthy subjects.

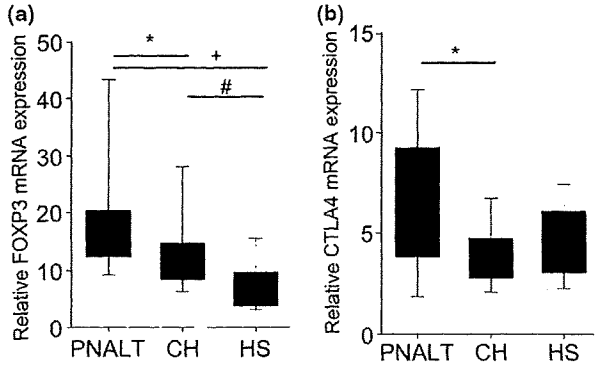

Fig. 2 Comparison of mRNA expression of FOXP3 and CTLA4 in CD4+CD25high+ T cells among the groups. The expression of FOXP3 (a) and CTLA4 (b) in separated CD4+CD25high+ T cells were analysed by real-time reverse transcriptase-polymerase chain reaction as described in Materials and methods. Boxes represent lower and upper quartiles with the median value (solid line) between boxes, while the whiskers represent the minimum and maximum values. *, $P < 0.05$; , $P < 0.01$; +, $P < 0.001$. For definitions of PNALT, CH and HS, see Fig. 1.

production stimulated with antigen-pulsed DC. We compared such responses between samples with or without CD4+CD25+ T cells. In PNALT patients, HCV NS5-specific T cell proliferation or IFN-γ production of CD25-depleted CD4+ T cells was significantly higher than those of the bulk CD4+ T cells (Fig. 3a,b). In contrast, in CH patients, such restoration did not occur significantly even when CD4+ CD25+ T cells had been depleted (Fig. 3a,b). There was no difference in the production of IL-10 and TGF-β between bulk CD4+ T cells and CD25-depleted CD4+ T cells in both CH and PNALT patients (Fig. 3c,d). These results suggest that co-existing CD4+CD25+ T cells play an inhibitory role in the HCV-specific CD4+ T cell response, in which suppression was more potent in the PNALT than in the CH group.

CD127–FOXP3+ cells, regardless of their CD25 expression, are increased in patients with HCV infection

In the analyses of N-Treg, the frequency of CD4+CD25–FOXP3+ T cells in HCV-infected patients was higher than those in the healthy donors (Fig. 1d). These results suggest that CD4+FOXP3+ T cells, regardless of the degree of CD25

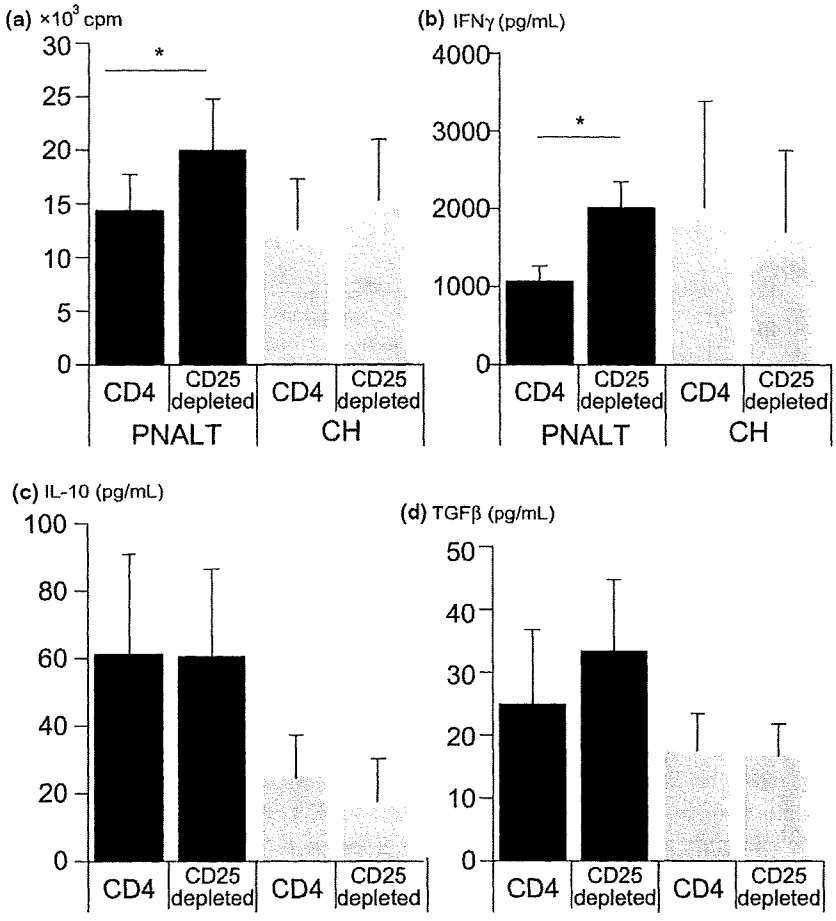

Fig. 3 Changes of hepatitis C virus (HCV)-specific CD4+ T cell responses with or without depletion of CD25+ T cells. Bulk CD4+ T cells or those depleted of CD25+ cells were cultured with autologous monocyte-derived dendritic cells in the presence of HCV-NS5 protein for 5 days as described in Materials and methods. (a) On day 4, [3H]-thymidine was pulsed and the thymidine incorporation was counted with a β-counter. Before the pulsing, the culture supernatants were harvested and subjected to enzyme-linked immunosorbent assay for interferon-γ (b), interleukin-10 (c) and TGF-β (d), respectively. *, $P < 0.05$ by Mann–Whitney *U*-test. For definitions of PNALT and CH, see Fig. 1.

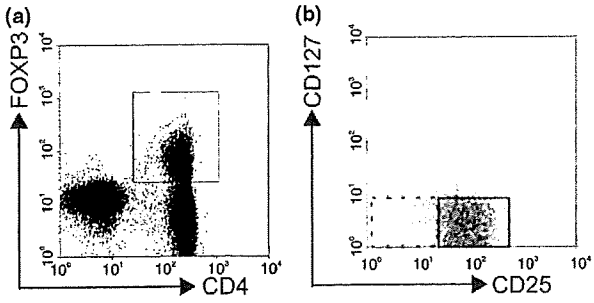

Fig. 4 Gating of CD4+CD127–FOXP3+ cells with variable CD25 expression under FACS analysis. After setting the gate on CD4+FOXP3+ cells [rectangle in the dot plot (a)], were displayed on the CD25 and CD127 axis (b). The presence of CD25+ (bold rectangle) and of CD25– cells (dotted rectangle) in CD4+FOXP3+ cells are shown in plot (b). The frequencies of these cells were analysed.

expression, increase in chronic HCV infection. Alternatively, it implies that higher expression of CD25 is not a universal marker for identifying FOXP3+ cells with regulatory activity. It has been reported that CD127 expression on CD4+ T cells is inversely correlated with FOXP3 expression, suggesting that CD127low/negative cells consist of those with regulatory activity. In order to analyse regulatory T cell subsets more precisely, we first examined FOXP3 expression on CD127– or CD127+ cells paired with CD25 expression in patients with HCV infection (Fig. 4). As a result, the majority of CD4+FOXP3+ T cells belonged to the CD127– population irrespective of CD25 expression (Fig. 4). Next, we compared the frequency of CD4+CD127–FOXP3+ cells, which consist of CD25+ and CD25– cells, among the subject groups (Fig. 5a). The frequency of CD4+CD127–FOXP3+ cells was similar in the CH and the PNALT groups, both of which were significantly higher than those in the HS (Fig. 5a). Finally, in order to estimate the profile of CD4+CD127–FOXP3+ cells according to CD25 expression, we compared the percentage of CD25+CD127–FOXP3+ or CD25–CD127–FOXP3+ cells in CD4+ T cells among the groups. The percentage of CD25+CD127–FOXP3+ T cells in CD4+ T cells was comparable for PNALT and CH (Fig. 5b). In clear contrast, the percentage of CD25–CD127–FOXP3+ T cells in the PNALT was lower than those in the CH (Fig. 5c). The frequencies of these cells were higher in the HCV-infected patients than in HS (Fig. 5b,c). When we set the focus on the proportion of CD25+CD127– or CD25-CD127– cells in the FOXP3+ cells in the periphery as a whole, we found that the proportion of CD25+CD127– cells in the PNALT was higher than that in the CH group (Fig. 5d). On the other hand, the proportion of CD25–CD127– cells in FOXP3+ cells was lower in the PNALT than in the CH group (Fig. 5e). Therefore, the phenotypic profiles of FOXP3+ T cells are distinct between PNALT and CH patients, with regard to the expression of CD127 and CD25.

DISCUSSION

Approximately 30–40% of chronically HCV-infected patients continue to display PNALT for decades. We previously reported the possible contribution of certain human leukocyte antigen haplotypes [23] or DC dysfunction in the maintenance of the PNALT state [24]. However, the precise mechanisms behind this important issue are yet to be

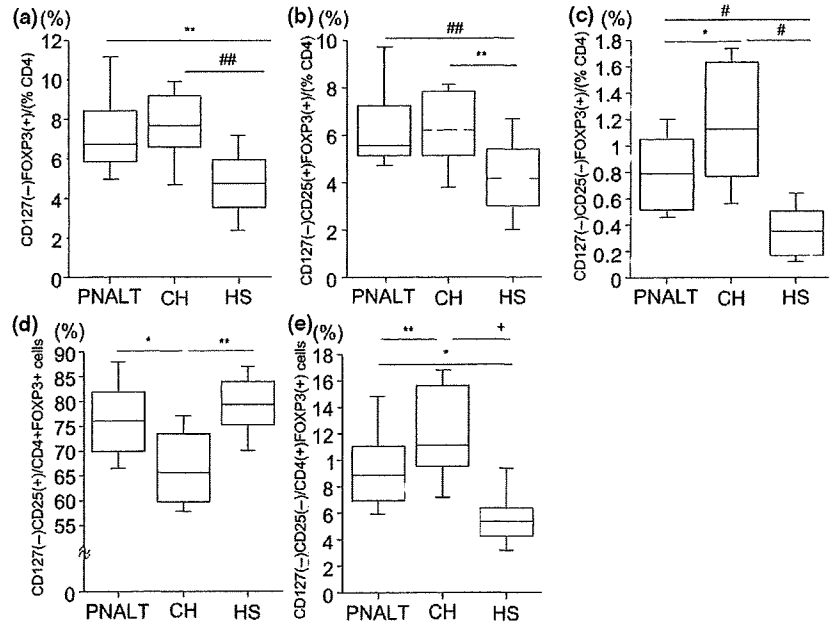

Fig. 5 Comparison in the frequencies of CD127– regulatory T cell subsets among the groups. Frequencies of CD127–FOXP3+ (a), CD127–CD25+FOXP3 (b) and CD127–CD25–FOXP3+ (c) cells among CD4+ T cells were determined by FACS analysis. The proportion of CD127–CD25+ (d) or CD127–CD25– (e) cells in CD4+FOXP3+ cells were also determined. Boxes represent lower and upper quartiles with the median value (solid line) between boxes, while the whiskers represent the minimum and maximum values. *, $P < 0.05$; , $P < 0.01$; **, $P < 0.005$; ##, $P < 0.001$; +, $P < 0.0001$ by Mann–Whitney *U*-test. For definitions of PNALT, CH and HS, see Fig. 1.

established. Cumulative reports have shown that Th1/Tc1 type responses are instrumental in HCV-induced liver inflammation [7,25,26]. We thus hypothesized that some suppressor mechanisms exist in PNALT patients especially against HCV-specific Th1 and/or CTL reactions.

The involvement of Treg cells in the pathogenesis of various diseases has been reported [9–13]. Most of the studies presented the possibility that N-Treg play substantial roles in the induction of tolerance against aetiological self or nonself antigens, thus leading to alleviation or exacerbation of the disease severity. With regard to HCV infection, several groups have shown that N-Treg are increased both in the periphery and in the liver and are able to inhibit HCV-specific CD4+ or CD8+ T cell responses *in vitro* [17,18,27]. In this study, we showed that the frequency of N-Treg in HCV-infected patients is higher than those in the controls, which is consistent with the previous reports. However, the frequencies of N-Treg are indistinguishable between the patient groups with different disease activities. As for the functional aspect, the deprivation of CD4+CD25+ cells enhanced the HCV NS5-specific CD4+ T cell response in the PNALT than in the CH group, suggesting that co-existing Treg in the PNALT are more suppressive. In addition, the expression of FOXP3 and CTLA4, which are key molecules of the suppressor function, is higher in PNALT than in those with active hepatitis. Venken *et al.* [28] demonstrated that the degree of FOXP3 expression at the single-cell level of N-Treg is well correlated with their suppressive ability, which is supportive of our results. In contrast, Bolacchi *et al.* [29] reported that the frequency of TGF-β+ N-Treg in the PNALT was higher than in the hepatitis group. Furthermore, their frequency was inversely correlated with the histological inflammatory grade, suggesting that TGF-β+ Treg play active roles in alleviating hepatitis. The reasons for the lack of correlation between N-Treg and serum ALT or HCV RNA quantity in the present study may be because of the difference in the target of analyses, such as either peripheral or intra-hepatic Treg, or either TGF-β+ or bulk Treg. Further analyses need to be performed on these important issues, as CD4+FOXP3+ Treg are reported to accumulate more in the portal tract of HCV-infected livers compared with those in the periphery [20].

During the observation period, about 30–40% of PNALT patients began to show elevated or fluctuating ALT abnormalities. What crucial factor triggers HCV-induced liver inflammation remains unknown. One of the plausible explanations is an antigenic shift accompanied by the occurrence of mutations in the HCV genome. In other words, hepatitis may flare up if the mutation raises HCV immunogenicity. Comprehensive analyses of HCV epitopes for CTL using overlapping peptides have shown that the HCV core and NS3 are more immunogenic than the remaining regions; however, the presence of an epitope hierarchy in Treg induction has been controversial. Li *et al.* [30] reported the possibility that Treg are expandable in response to certain epitopes in HCV proteins. In two patients in whom we observed flare-up of hepatitis in this study, we were able to find that the expression of FOXP3 in N-Treg was high in the PNALT status, but declined in the active hepatitis stage (data not shown). Although it is difficult to state whether such phenotypic changes in N-Treg are the cause or the consequence of disease progression, these results suggest the involvement of N-Treg in the degree of HCV-mediated hepatitis. Further detailed study is needed to examine whether or not such changes in N-Treg are related to the sequence evolution in HCV genomes.

Recent research has disclosed that distinct types of Treg are present in humans. Currently, it is generally accepted that CD25+FOXP3+ is the most reliable marker for Treg, which is induced in parallel with the acquisition of suppressor ability. However, owing to the lack of phenotypic markers for specifically identifying adaptive Treg, their roles in clinical settings have been unclear. In this study, CD4+FOXP3+ cells increased in HCV-infected patients, who were either positive or negative for CD25. In contrast to thymus-derived N-Treg expressing a greater degree of CD25, adaptive Treg are presumed to be induced in the periphery with a lesser degree of CD25 expression. Thus, it is likely that CD4+CD25–FOXP3+ T cells in HCV infection contain some part of adaptive Treg.

Treg have been reported to express low levels of CD127 at their cell surface [31]. Furthermore, the expression of CD127 is inversely correlated with FOXP3 expression and with the suppressive function of CD25high+ Treg. Liu *et al.* [22] pointed out the possibility that adaptive Treg are grouped into CD127– cells, which also include FOXP3-negative Tr1 or Th3 cells. Alternatively, You *et al.* [32] reported that murine CD4+CD25lowFOXP3+ T cells might be adaptive Treg, which exert a TGFβ-dependent suppressive function. Taking these reports into consideration, and in order to exclude activated CD25+ T cells, we examined CD4+CD127–CD25–FOXP3+ cells tentatively determined as part of adaptive Treg. In order to confirm that CD4+CD127– cells possess suppressive capacity, we co-cultured sorted CD4+CD127–CD25– or CD4+CD127–CD25+ cells with allogeneic CD4+ T cells stimulated with anti-CD3 and anti-CD28 antibodies. As a result, we found that CD4+CD127– cells, regardless of CD25 expression, significantly suppressed the proliferation of responder CD4+ T cells (manuscript in preparation). Of note is the finding that the frequency of CD127–CD25–FOXP3+ cells is higher in patients with active hepatitis than those in the PNALT group. One of the plausible explanations for such an increase of Treg is the compensatory mechanisms for the aggravation of liver inflammation. In support of this possibility, Bonelli *et al.* [33] reported that CD4+CD127–CD25– cells are increased in patients with systemic lupus erythematosus (SLE), the numbers of which are well correlated with disease activity. With regard to the ability of Treg in SLE patients, CD4+CD127–CD25– cells were potent in the inhibition of T

cell proliferation but not in IFN-γ release. Such a defective suppressor capacity may result in the continuation of tissue inflammation regardless of the presence of abundant Treg. The other conceivable role of CD4+CD25–CD127–FOXP3+ cells in active hepatitis may be a peripheral reservoir of CD4+CD25+FOXP3+ cells in case of flare-up of liver inflammation. In mice, it has been reported that CD25–FOXP3+ cells revert to CD25+FOXP3+ cells upon activation signals, thus leading to the expansion of the Treg pool [34]. In order to reach a definite conclusion on the role of CD127–CD25–FOXP3+ cells, further analyses are needed to elucidate whether these cells are inhibitory to either HCV-specific or HCV-nonspecific T cell responses.

Large-scale studies with HCV-infected patients demonstrated that the cumulative incidence of HCC in the PNALT group is extremely low compared with that in patients with apparent hepatitis and liver cirrhosis [35]. The lesser HCC incidence is also evident in patients who attained a lasting biochemical response to IFN-based therapy; even if they had failed to achieve sustained virological response [36]. These results clearly indicate that the maintenance of the PNALT state is one of the surrogate therapeutic goals in chronic HCV infection. Therefore, it is necessary to clarify the mechanisms of Treg induction in HCV infection, whether they are naturally or adaptively introduced, and to establish a feasible modality for controlling Treg. Our study has shown the importance of subset-oriented analyses of Treg for gaining access to that goal.

ACKNOWLEDGEMENT

This study was funded in part by Ministry of Education, Culture, Sports, Science and Technology, Ministry of Health, Labor and Welfare of Japan.

CONFLICT OF INTEREST

All of the authors do not have any commercial or other association that might pose a conflict of interest.

REFERENCES

1 Kasahara A, Hayashi N, Mochizuki K *et al.* Risk factors for hepatocellular carcinoma and its incidence after interferon treatment in patients with chronic hepatitis C. Osaka Liver Disease Study Group. *Hepatology* 1998; 27(5): 1394–1402.
2 Marcellin P, Levy S, Erlinger S. Therapy of hepatitis C: patients with normal aminotransferase levels. *Hepatology* 1997; 26 (3 Suppl. 1): 133S–136S.
3 Tassopoulos NC. Treatment of patients with chronic hepatitis C and normal ALT levels. *J Hepatol* 1999; 31 (Suppl. 1): 193–196.
4 Persico M, Persico E, Suozzo R *et al.* Natural history of hepatitis C virus carriers with persistently normal aminotransferase levels. *Gastroenterology* 2000; 118(4): 760–764.
5 Suruki R, Hayashi K, Kusumoto K *et al.* Alanine aminotransferase level as a predictor of hepatitis C virus-associated hepatocellular carcinoma incidence in a community-based population in Japan. *Int J Cancer* 2006; 119(1): 192–195.
6 Nelson DR, Marousis CG, Davis GL *et al.* The role of hepatitis C virus-specific cytotoxic T lymphocytes in chronic hepatitis C. *J Immunol* 1997; 158(3): 1473–1481.
7 Schirren CA, Jung MC, Gerlach JT *et al.* Liver-derived hepatitis C virus (HCV)-specific CD4(+) T cells recognize multiple HCV epitopes and produce interferon gamma. *Hepatology* 2000; 32(3): 597–603.
8 Sakaguchi S. Naturally arising CD4+ regulatory T cells for immunologic self-tolerance and negative control of immune responses. *Annu Rev Immunol* 2004; 22: 531–562.
9 Viglietta V, Baecher-Allan C, Weiner HL, Hafler DA. Loss of functional suppression by CD4+CD25+ regulatory T cells in patients with multiple sclerosis. *J Exp Med* 2004; 199(7): 971–979.
10 Ehrenstein MR, Evans JG, Singh A *et al.* Compromised function of regulatory T cells in rheumatoid arthritis and reversal by anti-TNFalpha therapy. *J Exp Med* 2004; 200(3): 277–285.
11 Sugiyama H, Gyulai R, Toichi E *et al.* Dysfunctional blood and target tissue CD4+CD25high regulatory T cells in psoriasis: mechanism underlying unrestrained pathogenic effector T cell proliferation. *J Immunol* 2005; 174(1): 164–173.
12 Weiss L, Donkova-Petrini V, Caccavelli L, Balbo M, Carbonneil C, Levy Y. Human immunodeficiency virus-driven expansion of CD4+CD25+ regulatory T cells, which suppress HIV-specific CD4 T-cell responses in HIV-infected patients. *Blood* 2004; 104(10): 3249–3256.
13 Ormandy LA, Hillemann T, Wedemeyer H, Manns MP, Greten TF, Korangy F. Increased populations of regulatory T cells in peripheral blood of patients with hepatocellular carcinoma. *Cancer Res* 2005; 65(6): 2457–2464.
14 Jonuleit H, Schmitt E. The regulatory T cell family: distinct subsets and their interrelations. *J Immunol* 2003; 171(12): 6323–6327.
15 Hori S, Nomura T, Sakaguchi S. Control of regulatory T cell development by the transcription factor Foxp3. *Science* 2003; 299(5609): 1057–1061.
16 Fontenot JD, Rudensky AY. A well adapted regulatory contrivance: regulatory T cell development and the forkhead family transcription factor Foxp3. *Nat Immunol* 2005; 6(4): 331–337.
17 Cabrera R, Tu Z, Xu Y *et al.* An immunomodulatory role for CD4(+)CD25(+) regulatory T lymphocytes in hepatitis C virus infection. *Hepatology* 2004; 40(5): 1062–1071.
18 Rushbrook SM, Ward SM, Unitt E *et al.* Regulatory T cells suppress *in vitro* proliferation of virus-specific CD8+ T cells during persistent hepatitis C virus infection. *J Virol* 2005; 79(12): 7852–7859.
19 Sugimoto K, Ikeda F, Stadanlick J, Nunes FA, Alter HJ, Chang KM. Suppression of HCV-specific T cells without differential hierarchy demonstrated *ex vivo* in persistent HCV infection. *Hepatology* 2003; 38(6): 1437–1448.
20 Ward SM, Fox BC, Brown PJ *et al.* Quantification and localisation of FOXP3+ T lymphocytes and relation to

hepatic inflammation during chronic HCV infection. *J Hepatol* 2007; 47(3): 316–324.
21 Chen W, Jin W, Hardegen N *et al.* Conversion of peripheral CD4+CD25– naive T cells to CD4+CD25+ regulatory T cells by TGF-beta induction of transcription factor Foxp3. *J Exp Med* 2003; 198(12): 1875–1886.
22 Liu W, Putnam AL, Xu-Yu Z *et al.* CD127 expression inversely correlates with FoxP3 and suppressive function of human CD4+ Treg cells. *J Exp Med* 2006; 203(7): 1701–1711.
23 Kuzushita N, Hayashi N, Moribe T *et al.* Influence of HLA haplotypes on the clinical courses of individuals infected with hepatitis C virus. *Hepatology* 1998; 27(1): 240–244.
24 Kanto T, Inoue M, Miyazaki M *et al.* Impaired function of dendritic cells circulating in patients infected with hepatitis C virus who have persistently normal alanine aminotransferase levels. *Intervirology* 2006; 49(1–2): 58–63.
25 Leroy V, Vigan I, Mosnier JF *et al.* Phenotypic and functional characterization of intrahepatic T lymphocytes during chronic hepatitis C. *Hepatology* 2003; 38(4): 829–841.
26 Penna A, Missale G, Lamonaca V *et al.* Intrahepatic and circulating HLA class II-restricted, hepatitis C virus-specific T cells: functional characterization in patients with chronic hepatitis C. *Hepatology* 2002; 35(5): 1225–1236.
27 Boettler T, Spangenberg HC, Neumann-Haefelin C *et al.* T cells with a CD4+CD25+ regulatory phenotype suppress *in vitro* proliferation of virus-specific CD8+ T cells during chronic hepatitis C virus infection. *J Virol* 2005; 79(12): 7860–7867.
28 Venken K, Hellings N, Thewissen M *et al.* Compromised CD4+ CD25(high) regulatory T-cell function in patients with relapsing-remitting multiple sclerosis is correlated with a reduced frequency of FOXP3-positive cells and reduced FOXP3 expression at the single-cell level. *Immunology* 2008; 123(1): 79–89.
29 Bolacchi F, Sinistro A, Ciaprini C *et al.* Increased hepatitis C virus (HCV)-specific CD4+CD25+ regulatory T lymphocytes and reduced HCV-specific CD4+ T cell response in HCV-infected patients with normal versus abnormal alanine aminotransferase levels. *Clin Exp Immunol* 2006; 144(2): 188–196.
30 Li S, Jones KL, Woollard DJ *et al.* Defining target antigens for CD25+ FOXP3+ IFN-gamma-regulatory T cells in chronic hepatitis C virus infection. *Immunol Cell Biol* 2007; 85(3): 197–204.
31 Seddiki N, Santner-Nanan B, Martinson J *et al.* Expression of interleukin (IL)-2 and IL-7 receptors discriminates between human regulatory and activated T cells. *J Exp Med* 2006; 203(7): 1693–1700.
32 You S, Leforban B, Garcia C, Bach JF, Bluestone JA, Chatenoud L. Adaptive TGF-beta-dependent regulatory T cells control autoimmune diabetes and are a privileged target of anti-CD3 antibody treatment. *Proc Natl Acad Sci USA* 2007; 104(15): 6335–6340.
33 Bonelli M, Savitskaya A, Steiner CW, Rath E, Smolen JS, Scheinecker C. Phenotypic and functional analysis of CD4+CD25– Foxp3+ T cells in patients with systemic lupus erythematosus. *J Immunol* 2009; 182(3): 1689–1695.
34 Zelenay S, Lopes-Carvalho T, Caramalho I, Moraes-Fontes MF, Rebelo M, Demengeot J. Foxp3+ CD25– CD4 T cells constitute a reservoir of committed regulatory cells that regain CD25 expression upon homeostatic expansion. *Proc Natl Acad Sci USA* 2005; 102(11): 4091–4096.
35 Okanoue T, Makiyama A, Nakayama M *et al.* A follow-up study to determine the value of liver biopsy and need for antiviral therapy for hepatitis C virus carriers with persistently normal serum aminotransferase. *J Hepatol* 2005; 43(4): 599–605.
36 Tanaka H, Tsukuma H, Kasahara A *et al.* Effect of interferon therapy on the incidence of hepatocellular carcinoma and mortality of patients with chronic hepatitis C: a retrospective cohort study of 738 patients. *Int J Cancer* 2000; 87(5): 741–749.

Mcl-1 and Bcl-xL Cooperatively Maintain Integrity of Hepatocytes in Developing and Adult Murine Liver

Hayato Hikita,[1]* Tetsuo Takehara,[1]* Satoshi Shimizu,[1] Takahiro Kodama,[1] Wei Li,[1] Takuya Miyagi,[1] Atsushi Hosui,[1] Hisashi Ishida,[1] Kazuyoshi Ohkawa,[1] Tatsuya Kanto,[1] Naoki Hiramatsu,[1] Xiao-Ming Yin,[2] Lothar Hennighausen,[3] Tomohide Tatsumi,[1] and Norio Hayashi[1]

Anti-apoptotic members of the Bcl-2 family, including Bcl-2, Bcl-xL, Mcl-1, Bcl-w and Bfl-1, inhibit the mitochondrial pathway of apoptosis. Bcl-xL and Mcl-1 are constitutively expressed in the liver. Although previous research established Bcl-xL as a critical apoptosis antagonist in differentiated hepatocytes, the significance of Mcl-1 in the liver, especially in conjunction with Bcl-xL, has not been clear. To examine this question, we generated hepatocyte-specific Mcl-1–deficient mice by crossing *mcl-1*$^{flox/flox}$ mice and *AlbCre* mice and further crossed them with *bcl-x*$^{flox/flox}$ mice, giving Mcl-1/Bcl-xL–deficient mice. The *mcl-1*$^{flox/flox}$ *AlbCre* mice showed spontaneous apoptosis of hepatocytes after birth, as evidenced by elevated levels of serum alanine aminotransferase (ALT) and caspase-3/7 activity and an increased number of terminal deoxynucleotidyl transferase-mediated 2′-deoxyuridine 5′-triphosphate nick-end labeling (TUNEL)-positive cells in the liver; these phenotypes were very close to those previously found in hepatocyte-specific Bcl-xL–deficient mice. Although *mcl-1*$^{flox/+}$ *AlbCre* mice did not display apoptosis, their susceptibility to Fas-mediated liver injury significantly increased. Further crossing of Mcl-1 mice with Bcl-xL mice showed that *bcl-x*$^{flox/+}$ *mcl-1*$^{flox/+}$ *AlbCre* mice also showed spontaneous hepatocyte apoptosis similar to Bcl-xL–deficient or Mcl-1–deficient mice. In contrast, *bcl-x*$^{flox/flox}$ *mcl-1*$^{flox/+}$ *AlbCre*, *bcl-x*$^{flox/+}$ *mcl-1*$^{flox/flox}$ *AlbCre*, and *bcl-x*$^{flox/flox}$ *mcl-1*$^{flox/flox}$ *AlbCre* mice displayed a decreased number of hepatocytes and a reduced volume of the liver on day 18.5 of embryogenesis and rapidly died within 1 day after birth, developing hepatic failure evidenced by increased levels of blood ammonia and bilirubin. *Conclusion:* Mcl-1 is critical for blocking apoptosis in adult liver and, in the absence of Bcl-xL, is essential for normal liver development. Mcl-1 and Bcl-xL are two major anti-apoptotic Bcl-2 family proteins expressed in the liver and cooperatively control hepatic integrity during liver development and in adult liver homeostasis in a gene dose-dependent manner. (HEPATOLOGY 2009;50:1217-1226.)

See Editorial on Page 1009

Abbreviations: ALT, alanine aminotransferase; PCR, polymerase chain reaction; RT-PCR, reverse transcription polymerase chain reaction; TNF-α, tumor necrosis factor alpha; TUNEL, terminal deoxynucleotidyl transferase-mediated 2′-deoxyuridine 5′-triphosphate nick-end labeling.

From the [1]Department of Gastroenterology and Hepatology, Osaka University Graduate School of Medicine, Osaka, Japan; the [2]Department of Pathology, University of Pittsburgh School of Medicine, Pittsburgh, PA; and the [3]Laboratory of Genetics and Physiology, National Institute of Diabetes and Digestive and Kidney Diseases, National Institutes of Health, Bethesda, MD.

**These authors contributed equally to this work and share first authorship.*

Received January 31, 2009; accepted June 8, 2009.

Supported in part by a Grant-in-Aid for Scientific Research from the Ministry of Education, Culture, Sports, Science, and Technology, Japan (to T.Tak.).

Address reprint requests to: Norio Hayashi, M.D., Ph.D., Department of Gastroenterology and Hepatology, Osaka University Graduate School of Medicine, 2-2 Yamadaoka, Suita, Osaka 565-0871, Japan. E-mail: hayashin@gh.med.osaka-u.ac.jp; fax:

Published online in Wiley InterScience (www.interscience.wiley.com).

DOI 10.1002/hep.23126

Potential conflict of interest: Nothing to report.

Additional Supporting Information may be found in the online version of this article.

The mitochondrial pathway of apoptosis is regulated by the Bcl-2 family proteins.[1,2] They are functionally divided into two basic groups: pro-apoptotic and anti-apoptotic members. Pro-apoptotic members are further divided into multi-domain members, such as Bax and Bak, and BH3-only proteins. Bax/Bak triggers release from mitochondria of cytochrome c, presumably by forming pores at the mitochondrial outer membrane. Cytochrome c released into the cytosol activates multiple caspases, which cut a variety of cellular substrates and dismantle the cell.[3] The release of Bax/Bak–mediated cytochrome c is considered to be a point of no return and a commitment to cell death.[4] Killing by BH3-only proteins, such as Bid, Bim, or Puma, requires Bax or Bak, placing them upstream of Bak/Bax activation. BH3-only proteins are transcriptionally or posttranslationally activated by a variety of cellular stresses. They are considered to be sensors that transmit apoptotic stimuli to mitochondria. Anti-apoptotic members, including Bcl-2, Bcl-xL, Mcl-1, Bcl-w, and Bfl-1, inhibit the mitochon-

drial pathway of apoptosis either by directly blocking Bak/Bax activation or by sequestering BH3-only proteins from Bak or Bax.

Mcl-1 has increasingly attracted attention because of its role in liver disease. Several reports have shown that Mcl-1 is overexpressed in a subset of human hepatocellular carcinomas and provides apoptosis resistance.[5-7] The multi-kinase inhibitor sorafenib, which was recently approved by the Food and Drug Administration as a chemotherapeutic agent for hepatocellular carcinoma,[8] is capable of down-regulating Mcl-1 expression and producing apoptosis in hepatoma cells.[9] Cycloxygenase 2 or hepatocyte growth factor up-regulates Mcl-1 expression in hepatocytes and improves Fas-mediated liver injury.[10,11] Recently, enforced expression of Mcl-1 was reported to reduce liver injury induced by anti-Fas injection in mice.[12] However, little is known about the physiologic significance of Mcl-1 in hepatocytes.

We previously reported that hepatocyte-specific Bcl-xL knockout mice were born and grew up but developed spontaneous hepatocyte apoptosis, identifying Bcl-xL as a critical apoptosis antagonist in hepatocytes.[13] This raises a question of whether other anti-apoptotic Bcl-2 family members, such as Mcl-1, have a significant role in regulating hepatocyte apoptosis and what the relationship is among those molecules. To this end, in the current study, we generated hepatocyte-specific Mcl-1 knockout as well as Bcl-xL/Mcl-1 double knockout mice and found that, like Bcl-xL, Mcl-1 is critical for maintaining hepatocyte integrity in adult liver, but not essential for liver development. However, both deficiencies cause a severe defect in liver development and lethality during the early neonatal period because of severe hepatic failure. The current study identifies Bcl-xL and Mcl-1 as two major anti-apoptotic Bcl-2 family proteins in the liver and demonstrates their gene dose–dependent effects for controlling hepatic integrity.

Materials and Methods

Mice. Mice carrying the *mcl-1* gene encoding amino acids 1 through 179 flanked by 2 *lox*P (*mcl-1*$^{flox/flox}$) were provided by Dr. You-Wen He of Duke University.[14] Mice carrying a *bcl-x* gene with two *lox*P sequencers at the promoter region and a second intron (*bcl-x*$^{flox/flox}$) were described previously.[15] Heterozygous AlbCre transgenic mice expressing Cre recombinase gene under the promoter of the albumin gene were described previously.[13] We generated hepatocyte-specific Mcl-1 knockout mice (*mcl-1*$^{flox/flox}$ *AlbCre*) by mating *mcl-1*$^{flox/flox}$ and *AlbCre* mice. We then used these knockout mice to generate hepatocyte-specific Bcl-xL/Mcl-1 knockout mice (*bcl-x*$^{flox/flox}$ *mcl-1*$^{flox/flox}$ *AlbCre*) by mating them with *bcl-x*$^{flox/flox}$ mice. Traditional Bid knockout mice were described previously.[16] They were maintained in a specific pathogen–free facility and treated with humane care under approval from the Animal Care and Use Committee of Osaka University Medical School.

Genotyping. Genomic DNA was extracted from the tail and subjected for polymerase chain reaction (PCR) for genotyping mice. The primers used were as follows: 5′-GCCACCTCATCAGTCGGG-3′ and 5′-TCAGAAGCCGCAATATCCCC-3′ for the *bcl-x* allele; 5′-GGTTCCCTGTCTCCTTACTTACTGTAG-3′ and 5′-CTCCTAACCACTGTTCCTGACATCC-3′ for the *mcl-1* allele; 5′-GCGGTCTGGCAGTAAAAACTATC-3′, 5′-GTGAAACAGCATTGCTGTCACTT-3′, 5′CTAGGCCACAGAATTGAAAGATCT-3′ 5′-GTAGGTGGAAATTCTAGCATCATCC-3′ for the *AlbCre* allele; 5′-CCGAAA TGTCCCATAAGAG-3′, 5′-GAGATGGACCACAACATC-3′, and 5′ TGCTACTTCCATTTGTCACGTCCT-3′ for the *bid* allele. PCR products were electrophoretically separated using 2% agarose gels. The expected sizes of the PCR products were as follows: 165 bp for the wild-type *bcl-x* allele, 195 bp for the floxed *bcl-x* allele, 200 bp for the wild-type *mcl-1* allele, 300 bp for the floxed *mcl-1* allele, 130 bp for the wild-type *bid* allele, and 350 bp for the *bid* knockout allele. *AlbCre*-negative mice showed a 350-bp band, and heterozygous *AlbCre* mice showed 100-bp and 350-bp double bands.

Apoptosis Assay. To measure serum ALT level and caspase-3/7 activity, blood was collected from the inferior vena cava of mice and centrifuged. Serum was stored at −20°C until use. Serum ALT levels were measured by a standard method at Oriental Kobo Life Science Laboratory (Nagahama, Japan), and serum caspase-3/7 activity was measured by a luminescent substrate assay for caspase-3 and caspase-7 (Caspase-Glo assay, Promega, Tokyo, Japan). For histological analysis, livers were formalin-fixed, embedded in paraffin, and thin sliced. The liver sections were stained with hematoxylin-eosin. To detect cells with oligonucleosomal DNA breaks, the sections were also subjected to terminal deoxynucleotidyl transferase-mediated 2′-deoxyuridine 5′-triphosphate nick-end labeling (TUNEL) staining, according to a previously reported procedure.[17] For Fas-stimulating study, anti-Fas antibody (Jo2 clone) (PharMingen, San Diego, CA) was intraperitoneally injected into mice 3 hours before sacrifice.

Western Blot Analysis. Approximately 25 mg liver tissues was lysed with a lysis buffer (1% NP-40, 0.5%

sodium deoxycholate, 0.1% sodium dodecyl sulfate and 1× protein inhibitor cocktail (Nacalai tesque, Kyoto, Japan), phosphate-buffered saline; pH 7.4). After incubation on ice for 15 minutes, the lysate was centrifuged at 10,000*g* for 15 minutes at 4°C. The protein content of the supernatants was determined using a bicinchoninic acid protein assay kit (Pierce, Rockford, IL). Equal amounts of protein were electrophoretically separated by sodium dodecyl sulfate polyacrylamide gels (8% or 12%) and transferred onto polyvinylidene fluoride membrane. For immunodetection, the following antibodies were used: anti–Bcl-xL antibody (Santa Cruz Biotechnology, Santa Cruz, CA), anti–Mcl-1 antibody (Rockland, Gilbertsville, PA), anti-Bax antibody (Cell Signaling Technology, Beverly, MA), anti-Bid antibody (Cell Signaling Technology), anti-albumin antibody (Affinity Bioreagents, Golden, CO), and anti–beta actin antibody (Sigma-Aldrich, Saint Louis, MO). Detection of immunolabeled proteins was performed using a chemiluminescent substrate (Pierce).

Neonate Analysis. Neonatal mice delivered by cesarean section were suckled by a surrogate mother and sacrificed at 10 hours after birth. Blood from the neonatal mice was centrifuged, and the plasma was stored at −20°C until use. The levels of total bilirubin and ammonia were measured by Van den Bergh reaction and a standard enzymatic procedure, respectively, at Oriental Kobo Life Science Laboratory.

Real-Time Reverse-Transcription PCR. Total RNA was prepared from liver tissue using RNeasy kit (QIAGEN, Tokyo, Japan). For complementary DNA synthesis, 1 μg total RNA was reverse-transcribed using the High Capacity RNA-to-DNA Master Mix (Applied Biosystems, Foster City, CA). Complementary DNA, equivalent to 40 ng RNA, was used as a template for real-time reverse-transcription PCR (RT-PCR) using an Applied Biosystems 7900HT Fast Real-Time PCR System (Applied Biosystems). The messenger RNA expressions of tumor necrosis factor alpha (TNF-α), collagen-alpha1(I), and transthyretin were measured using TaqMan Gene Expression Assays (Assay ID: Mm00443260_g1, Mm00801666_g1, and Mm00443267_m1, respectively), and were corrected with the quantified expression level of beta-actin messenger RNA measured using TaqMan Gene Expression Assays (Assay ID: Mm02619580_g1).

Statistical Analysis. Data are presented as mean ± standard deviation. Comparisons between two groups were performed by unpaired *t* test. Multiple comparisons were performed by analysis of variance followed by Scheffe *post hoc* correction. $P < 0.05$ was considered statistically significant.

Results

Hepatocyte-Specific Mcl-1 Deficiency Leads to Spontaneous Hepatocyte Apoptosis in the Adult Liver. To generate hepatocyte-specific Mcl-1–deficient mice, floxed *mcl-1* mice were crossed with heterozygous *AlbCre* mice. After *mcl-1*$^{flox/+}$ *AlbCre* mice were mated with *mcl-1*$^{flox/+}$ mice, and offspring were screened for genotyping and Mcl-1 expression. *mcl-1*$^{flox/flox}$ *AlbCre* mice were born and grew up. Their expression in the liver of Mcl-1 was greatly reduced compared with that of wild-type mice (Fig. 1A). The levels of Bcl-xL expression did not change in *mcl-1*$^{flox/flox}$ *AlbCre* liver. Bcl-xL and Mcl-1 proteins migrated as typical doublet bands of which the biochemical nature had been previously determined.[18] The trace amount of Mcl-1 expression found in the knockout liver may have been attributable to expression in nonparenchymal cells, as previously observed in hepatocyte-specific Bcl-xL–deficient mice.[13]

To investigate the significance of Mcl-1 in the liver, mice were sacrificed 6 weeks after birth and subjected to analysis of serum ALT levels and caspase-3/7 activity as well as liver histology and TUNEL staining. *mcl-1*$^{flox/flox}$ *AlbCre* mice displayed significantly higher levels of serum ALT than control mice (*AlbCre*-negative or *mcl-1*$^{+/+}$ *AlbCre* mice) (Fig. 1B). Hepatocytes with typical apoptosis morphology such as cellular shrinkage and nuclear condensation were frequently observed in the liver sections of *mcl-1*$^{flox/flox}$ *AlbCre* mice (Fig. 1C). Consistently, the number of cells with TUNEL positivity, a hallmark of apoptotic cell death, in the liver was significantly higher in *mcl-1*$^{flox/flox}$ *AlbCre* mice than in control mice (Fig. 1C). Activity of caspase-3/7, executioners of apoptosis, was significantly higher in circulation of *mcl-1*$^{flox/flox}$ *AlbCre* mice than in control mice, which might reflect activation of those proteases in the knockout liver (Fig. 1D). Bax expression was clearly increased in *mcl-1*$^{flox/flox}$ *AlbCre* mice, suggesting Bax activation being involved in the apoptosis in *mcl-1*$^{flox/flox}$ *AlbCre* mice (Fig. 1A). Furthermore, the expression of TNF-α and collagen-alpha1(I) was significantly increased in the *mcl-1*$^{flox/flox}$ *AlbCre* liver compared with the wild-type liver, as found in the Bcl-xL knockout liver (Fig. 1E). Taken together, hepatocyte-specific Mcl-1 knockout mice developed spontaneous apoptosis leading to sterile inflammation and fibrotic response in the liver, like hepatocyte-specific Bcl-xL knockout mice.[13]

Heterozygous Deletion of the mcl-1 Gene Does Not Produce Apoptosis But Increases the Susceptibility to Fas Stimulation. Although the levels of Mcl-1 expression were significantly decreased in *mcl-1*$^{flox/+}$ *AlbCre* liver (Fig. 1A, Supporting Fig. 1), *mcl-1*$^{flox/+}$ *AlbCre* mice did not have apoptosis phenotypes in the liver (Fig. 1B-D).

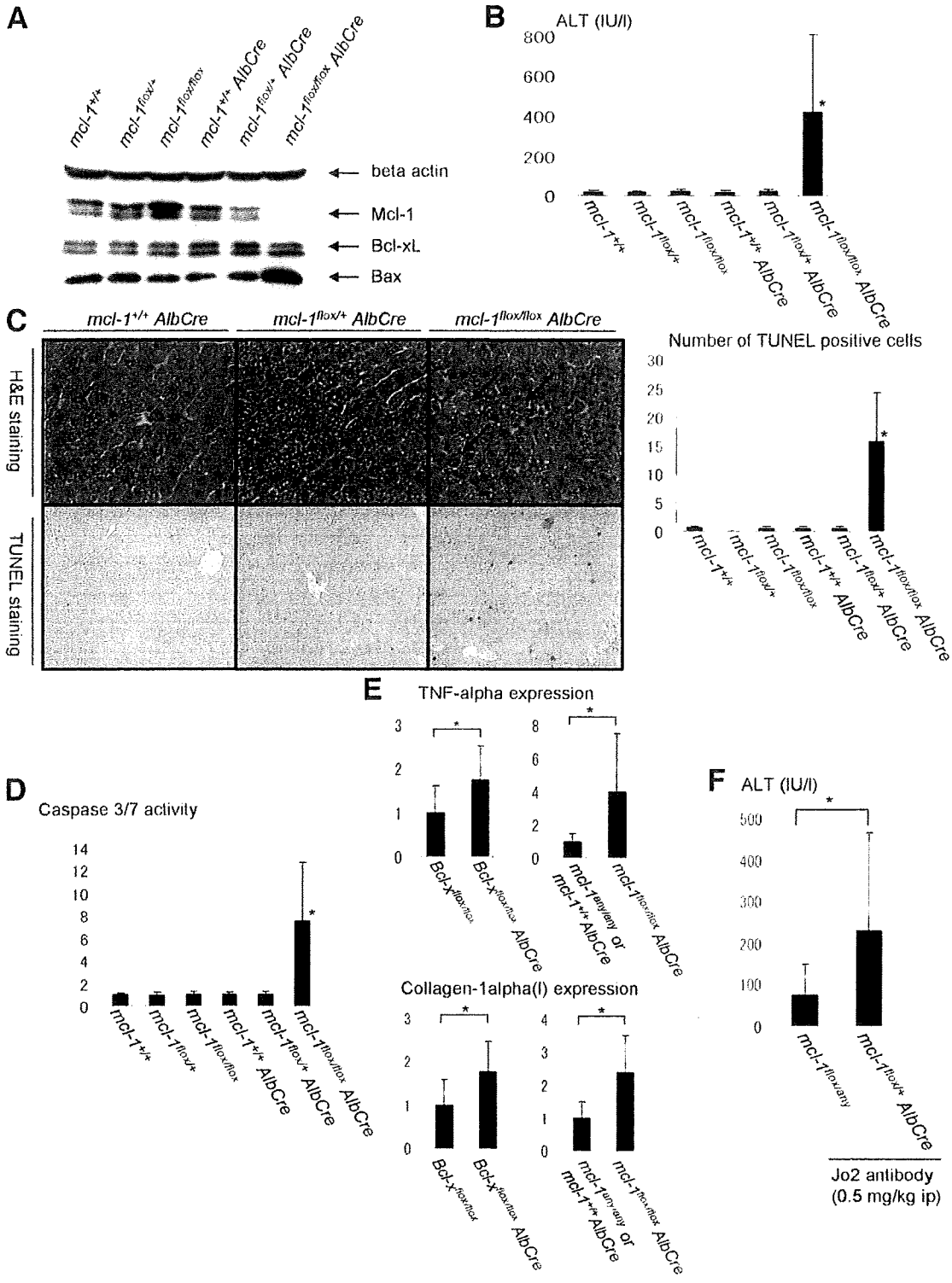

Fig. 1. Hepatocyte-specific Mcl-1 knockout mice. Offspring from mating of *mcl-1*$^{flox/+}$ *AlbCre* mice and *mcl-1*$^{flox/+}$ mice were sacrificed at the age of 6 weeks. (A) Western blot of whole liver lysate for the expression of Bcl-xL, Mcl-1, and Bax. (B) Serum ALT levels. N = 15 mice for each group. *$P < 0.05$ versus the other five groups. (C) Left panel shows hematoxylin-eosin and TUNEL staining of the liver section. Arrow indicates typical apoptotic cells. Right panel shows statistics of TUNEL-positive cells. The number of TUNEL-positive cells was determined in a defined area. N = 5 mice for each group. *$P < 0.05$ versus the other five groups. (D) Serum levels of caspase-3/7 activity. The levels were normalized to *mcl-1*$^{+/+}$ *AlbCre* (−) mice. N = 15 mice for each group. *P < 0.05 versus the other five groups. (E) Real-time RT-PCR analysis for TNF-α and collagen-1alpha(1) expression. *$P < 0.05$. N = 12 or 9. The levels were normalized to the wild-type mice. (F) Serum ALT levels of Fas-stimulated mice. The *mcl-1*$^{flox/+}$ *AlbCre* mice and *mcl-1*$^{flox/+\ or\ flox}$ mice were sacrificed 3 hours after intraperitoneal injection of 0.5 mg/kg Jo2 antibody. *$P < 0.05$. N = 13 or 7.

Therefore, we examined the susceptibility to Fas stimulation in these mice. We injected anti-Fas antibody into *mcl-1*$^{flox/+}$ *AlbCre* mice and *mcl-1*$^{flox/+\ or\ flox}$ mice and measured the levels of their serum ALT. *mcl-1*$^{flox/+}$ *AlbCre* mice displayed significantly higher levels of serum ALT than control mice (Fig. 1F). These findings suggest that haplo-deficiency of Mcl-1 does not produce apoptosis in a physiological setting but clearly reduces apoptosis resistance under pathological conditions.

Involvement of Bid in Apoptosis Caused by Mcl-1 Deficiency. BH3-only proteins regulate life and death balance by interacting with core Bcl-2 family members. The hepatocyte is a so-called type 2 cell, which requires Bid as a sensor for Fas-mediated apoptotic stresses.[19] In addition, it has been reported that the caspase-8/Bid pathway is involved in a variety of liver pathological conditions.[16,20] To examine the possibility of Bid being involved in hepatocyte apoptosis caused by Mcl-1 deficiency, we crossed hepatocyte-specific Mcl-1 knockout mice with Bid knockout mice. Offspring form mating of *bid*$^{+/-}$ *mcl-1*$^{flox/flox}$ *AlbCre* mice with *bid*$^{+/-}$ *mcl-1*$^{flox/flox}$ mice were sacrificed at 6 weeks after birth and subjected to analysis of apoptosis phenotypes. Mice with each genotype grew up, and, as expected, the levels of Bid and/or Mcl-1 expression in the liver were correspondingly reduced with their genotypes (Fig. 2A). The levels of serum ALT were significantly lower in *bid*$^{-/-}$ *mcl-1*$^{flox/flox}$ *AlbCre* mice than in *bid*$^{+/+}$ *mcl-1*$^{flox/flox}$ *AlbCre* mice (Fig. 2B). The results indicate that Bid was involved in hepatocyte apoptosis found in Mcl-1 knockout mice.

Combined Deficiency of Mcl-1 and Bcl-xL in Hepatocytes Causes Lethality. Phenotypes observed in hepatocyte-specific Mcl-1 knockout mice were very similar to those in hepatocyte-specific Bcl-xL knockout mice.[13] These results indicated that Bcl-xL and Mcl-1 share similar anti-apoptotic functions but do not compensate for the loss of each other. To examine whether their expression and function are completely nonredundant or just partially so, we generated hepatocyte-specific Bcl-xL/Mcl-1 double-knockout mice.

The *bcl-x*$^{flox/+}$ *mcl-1*$^{flox/+}$ *AlbCre* mice were mated with *bcl-x*$^{flox/flox}$ *mcl-1*$^{flox/flox}$ mice, and genotypes of the offspring were screened at 3 weeks after birth. *AlbCre*-negative and *bcl-x*$^{flox/+}$ *mcl-1*$^{flox/+}$ *AlbCre* mice were born and grew up, but not *bcl-x*$^{flox/flox}$ *mcl-1*$^{flox/+}$ *AlbCre*, *bcl-x*$^{flox/+}$ *mcl-1*$^{flox/flox}$ *AlbCre*, and *bcl-x*$^{flox/flox}$ *mcl-1*$^{flox/flox}$ *AlbCre* mice (Table 1). The lack of Bcl-xL and Mcl-1 caused a more severe phenotype than either knockout, suggesting that they partially compensate for the loss of each other at least from the viewpoint of maintaining normal development.

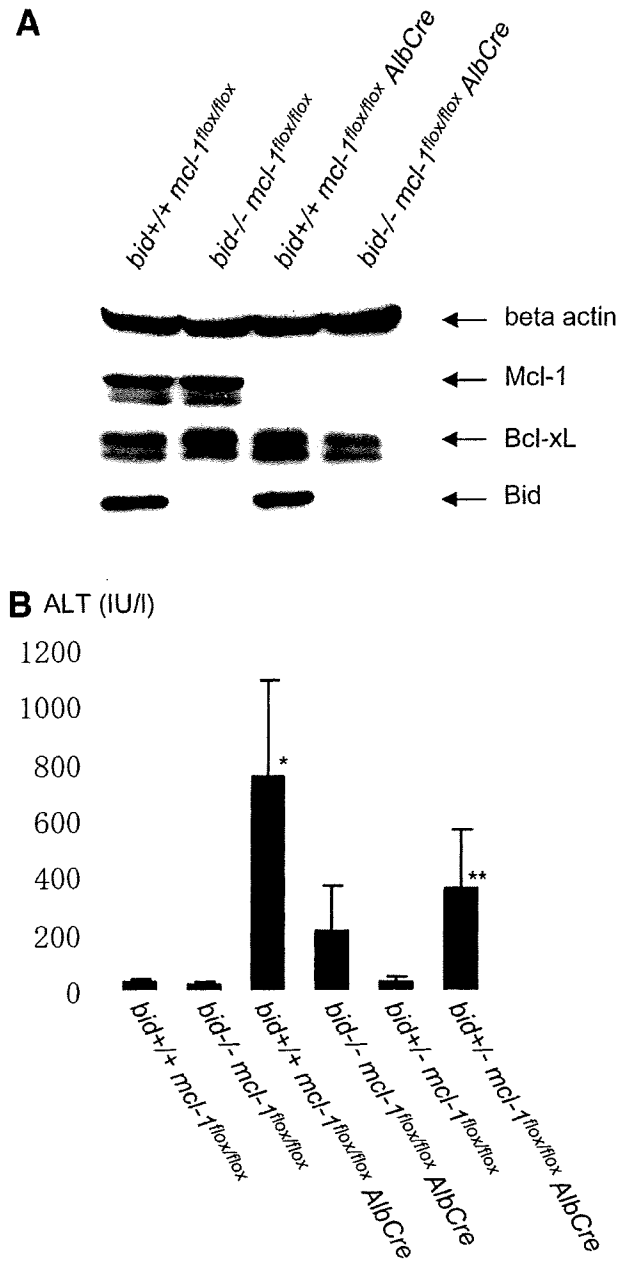

Fig. 2. Mcl-1/Bid double-knockout mice. Offspring from mating of *bid*$^{+/-}$ *mcl-1*$^{flox/flox}$ *AlbCre* mice with *bid*$^{+/-}$ *mcl-1*$^{flox/flox}$ mice were sacrificed at 6 weeks after birth. (A) Western blot of whole liver lysate for the expression of Mcl-1, Bcl-xL, and Bid. (B) Serum ALT levels. N = 12 mice for each group. *$P < 0.05$ versus the other five groups; **$P < 0.05$ versus the *AlbCre*-negative groups and the *bid*$^{+/+}$ *mcl-1*$^{flox/flox}$ *AlbCre* group.

Mice Lacking Single Alleles for Both Bcl-xL and Mcl-1 Develop Spontaneous Apoptosis in the Adult Liver Similar to Bcl-xL or Mcl-1 Knockout Mice. Offspring from mating of *bcl-x*$^{flox/+}$ *mcl-1*$^{flox/+}$ *AlbCre and bcl-x*$^{flox/flox}$ *mcl-1*$^{flox/flox}$ were sacrificed at 6 weeks after birth and subjected to analysis of Bcl-xL/Mcl-1 expression and

Table 1. Genotyping of Offspring Obtained by Crossing *bcl-x*$^{flox/+}$ *mcl-1*$^{flox/+}$ *AlbCre* Mice and *bcl-x*$^{flox/flox}$ *mcl-1*$^{flox/flox}$ Mice

AlbCre	bcl-x	mcl-1	ED18.5	3 Weeks
−	flox/+	flox/+	4	14
−	flox/flox	flox/+	6	17
−	flox/+	flox/flox	12	17
−	flox/flox	flox/flox	7	17
+	flox/+	flox/+	11	22
+	flox/flox	flox/+	8	0
+	flox/+	flox/flox	9	0
+	flox/flox	flox/flox	10	0
	Total		67	87

ED, embryonic day.

Note that each genotype is expected to account for one-eighth of the offspring from this mating.

apoptosis phenotypes. As expected, *bcl-x*$^{flox/+}$ *mcl-1*$^{flox/+}$ *AlbCre* liver expressed reduced levels of expression for both Bcl-xL and Mcl-1 (Fig. 3A). Interestingly, *bcl-x*$^{flox/+}$ *mcl-1*$^{flox/+}$ *AlbCre* mice developed spontaneous hepatocyte apoptosis as evidenced by an increase in serum ALT levels and caspase-3/7 activity (Fig. 3B,C). In agreement with this, hepatocytes with typical apoptotic morphology and positive for TUNEL staining were found scattered in the liver lobules in these mice (Fig. 3D,E). Furthermore, *bcl-x*$^{flox/+}$ *mcl-1*$^{flox/+}$ *AlbCre* mice showed higher expression of TNF-α than wild-type mice (Fig. 3F). The phenotypes were very similar to hepatocyte-specific Bcl-xL or Mcl-1knockout mice.

Hepatocyte-Specific Mcl-1/Bcl-xL-Deficient Mice Show Impaired Development of the Liver and Liver Failure During the Neonatal Period. To examine the impact of Bcl-xL/Mcl-1deficiency at an earlier time point, offspring obtained from crossing *bcl-x*$^{flox/+}$ *mcl-1*$^{flox/+}$ *AlbCre* mice and *bcl-x*$^{flox/flox}$ *mcl-1*$^{flox/flox}$ mice were analyzed on gestational day 18.5. Live-obtained embryo followed expected Mendelian frequencies (Table 1). Overall, they looked normal, and their body weight did not differ among genotypes (Fig. 4A,B). However, the livers obtained from live pups with genotype of *bcl-x*$^{flox/flox}$ *mcl-1*$^{flox/+}$ *AlbCre*, *bcl-x*$^{flox/+}$ *mcl-1*$^{flox/flox}$ *AlbCre*, or *bcl-x*$^{flox/flox}$ *mcl-1*$^{flox/flox}$ *AlbCre* were clearly smaller. The ratios of liver weight to body weight were significantly lower in those pups than in *AlbCre*-negative or *bcl-x*$^{flox/+}$ *mcl-1*$^{flox/+}$ *AlbCre* pups (Fig. 4C). The ratios of liver weight to body weight were also examined in *mcl-1*$^{flox/flox}$ with *AlbCre* or without *AlbCre* mice, and there was no significant difference between the two (6.0 ± 0.8 versus 5.5 ± 0.9, $N = 5$, $P = 0.34$), excluding the possibility that Mcl-1 knockout itself affects the liver size at this time point. Histological analysis revealed that there were a number of hepatocytes with rectangular morphology and hematopoietic cells in the developing liver of the *AlbCre*-negative pups (Fig. 4D). Whereas the number of rectangular hepatocytes in *bcl-x*$^{flox/+}$ *mcl-1*$^{flox/+}$ *AlbCre* livers was similar to that in the *AlbCre*-negative livers, it was lower in *bcl-x*$^{flox/flox}$ *mcl-1*$^{flox/+}$ *AlbCre*, *bcl-x*$^{flox/+}$ *mcl-1*$^{flox/flox}$ *AlbCre*, and *bcl-x*$^{flox/flox}$ *mcl-1*$^{flox/flox}$ *AlbCre* livers. Rectangular cells were rarely observed in *bcl-x*$^{flox/flox}$ *mcl-1*$^{flox/flox}$ *AlbCre* livers. Furthermore, the expression of albumin and transthyretin was examined in the liver as a marker for hepatocyte differentiation.[21] Consistent with histological findings, both expressions were gradually reduced from the *AlbCre*-negative livers to the *bcl-x*$^{flox/flox}$ *mcl-1*$^{flox/flox}$ *AlbCre* livers (Fig. 4E,F).

We noticed that offspring obtained from crossing *bcl-x*$^{flox/+}$ *mcl-1*$^{flox/+}$ *AlbCre* mice and *bcl-x*$^{flox/flox}$ *mcl-1*$^{flox/flox}$ mice frequently died within 1 day after birth. To examine the cause of the early neonatal death, offspring were sacrificed at 10 hours after birth. They were divided into two groups according to the data shown in Table 1: expected survivors including *AlbCre*-negative and *bcl-x*$^{flox/+}$ *mcl-1*$^{flox/+}$ *AlbCre* pups, and expected nonsurvivors including *bcl-x*$^{flox/flox}$ *mcl-1*$^{flox/+}$ *AlbCre*, *bcl-x*$^{flox/+}$ *mcl-1*$^{flox/flox}$ *AlbCre*, and *bcl-x*$^{flox/flox}$ *mcl-1*$^{flox/flox}$ *AlbCre* pups. The levels of total bilirubin and ammonia in circulation were determined and compared between the groups. Both blood bilirubin levels and ammonia levels were significantly higher in the expected nonsurvivors than in the expected survivors (Fig. 5A,B). These results suggested that *bcl-x*$^{flox/flox}$ *mcl-1*$^{flox/+}$ *AlbCre*, *bcl-x*$^{flox/+}$ *mcl-1*$^{flox/flox}$ *AlbCre*, and *bcl-x*$^{flox/flox}$ *mcl-1*$^{flox/flox}$ *AlbCre* mice died quickly after birth because of hepatic failure, in agreement with the findings of impaired liver development.

Discussion

Five members of the anti-apoptotic Bcl-2 family have been found: Bcl-2, Bcl-xL, Bcl-w, Bfl-1, and Mcl-1. Traditional knockout of Bcl-2, a prototype of this family, displays growth retardation, hair color abnormality, lymphocyte decrease, and polycystic kidney.[22,23] In agreement with the finding that Bcl-2 is not expressed in hepatocytes,[13] these mice did not show any liver phenotypes. Similarly, Bcl-w[24,25] or Bfl-1 knockout mice[26] were generated but no liver phenotypes have been reported. Traditional knockout of Bcl-xL or Mcl-1 caused more severe phenotypes. Deletion of the *bcl-x* gene resulted in embryonic lethality because of abnormal neuronal development and hematopoiesis.[27] The *mcl-1* knockout embryo fails to be implanted *in utero*.[28] Thus, study of traditional knockout mice could not reveal the significance of Bcl-xL or Mcl-1 in the liver.

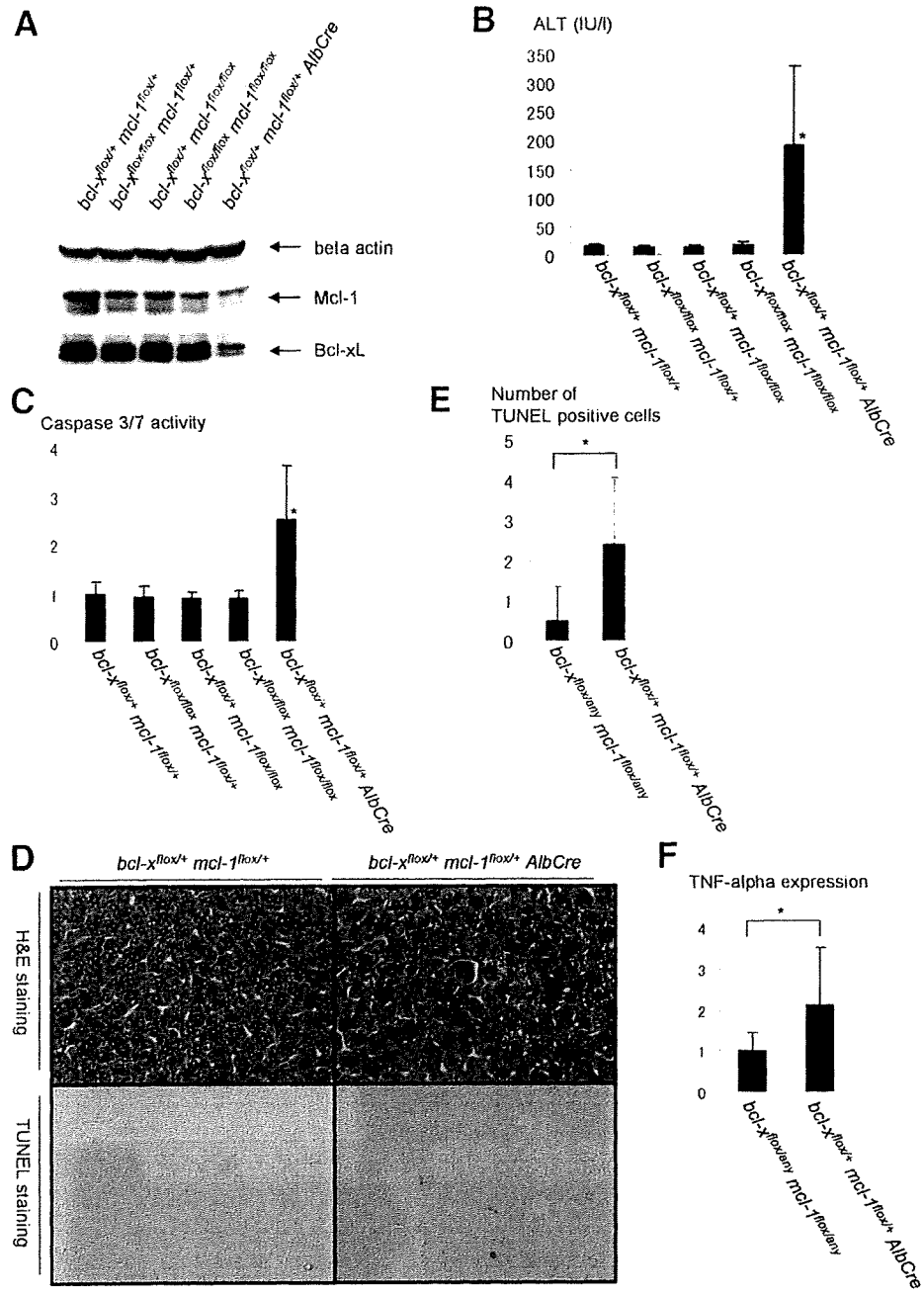

Fig. 3. Hepatocyte-specific Bcl-xL/Mcl-1-deficient mice. Offspring from mating *bcl-x*$^{flox/+}$ *mcl-1*$^{flox/+}$ *AlbCre* mice and *bcl-x*$^{flox/flox}$ *mcl-1*$^{flox/flox}$ mice were sacrificed at the age of 6 weeks. (A) Western blot of whole liver lysate for the expression of Bcl-xL and Mcl-1. (B) Serum ALT levels. N = 9 mice for each group. *$P < 0.05$ versus the other five groups. (C) Serum levels of caspase-3/7 activity. The levels were normalized to *bcl-x*$^{flox/+}$ *mcl-1*$^{flox/+}$ mice. N = 9 mice for each group. *$P < 0.05$ versus the other five groups. (D) Hematoxylin-eosin and TUNEL staining of the liver sections for *bcl-x*$^{flox/+}$ *mcl-1*$^{flox/+}$ *AlbCre* mice. Findings for *bcl-x*$^{flox/+}$ *mcl-1*$^{flox/+}$ mice are shown as a control. (E) Statistics of TUNEL-positive cells. The number of TUNEL-positive cells was determined in a defined area. N = 5 or 6. *$P < 0.05$. (F) RT-PCR analysis for TNF-α expression. The levels were normalized to the group of *bcl-x*$^{flox/+ \text{ or } flox}$ *mcl-1*$^{flox/+ \text{ or } flox}$. *$P < 0.05$. N = 9.

We previously reported that hepatocyte-specific knockout of Bcl-xL caused spontaneous apoptosis in hepatocytes after birth and established that Bcl-xL is critically important for the integrity of hepatocytes.[13] The current study demonstrated that Mcl-1 plays an anti-apoptotic role in differentiated hepatocytes similar to that of Bcl-xL. During the preparation of this manuscript, a report by Vick et al.[29] appeared on the Web, demonstrating a similar apoptosis phenotype in mice with specific knockout of the *mcl-1* gene in hepatocytes. Our findings